ARMY RESEARCH LABORATORY

Design Procedure for a Frequency-Scanned Traveling Wave Antenna, Part I: Air-Filled Waveguide

William Coburn and Wasyl Wasylkiwskyj

ARL-TR-791 September 2001

The findings in this report are not to be construed as an official Department of the Army position unless so designated by other authorized documents.

Citation of manufacturer's or trade names does not constitute an official endorsement or approval of the use thereof.

Destroy this report when it is no longer needed. Do not return it to the originator.

Army Research Laboratory

Adelphi, MD 20783-1197

ARL-TR-791 **September 2001**

Design Procedure for a Frequency-Scanned Traveling Wave Antenna, Part I: Air-Filled Waveguide

William Coburn

Sensors and Electron Devices Directorate, ARL

Wasyl Wasylkiwskyj

George Washington University

Abstract

A leaky waveguide antenna is investigated through a combination of theoretical analysis and numerical simulation. We developed a design procedure based on the analysis of Goldstone and Oliner, for an aperture in the narrow wall of a rectangular waveguide. We can phase scan the antenna by adjusting the propagation constant of the guiding structure, and we can frequency scan it by taking advantage of a frequency dispersive behavior. A combination of frequency and phase scanning can be used to steer the beam. We describe how the aperture illumination function is synthesized for a constant width aperture and we present the design equations. We use a numerical simulation of the leaky waveguide section to obtain the radiation efficiency. We then calculate the realized gain to evaluate the frequency scan range and radiation pattern characteristics. The results demonstrate that the main beam position can be scanned in the range of 10° to 30° from broadside over a narrow frequency range without corrupting the radiation pattern.

Contents

Figures

1. Introduction

A traveling wave antenna (TWA) is one for which the fields and currents producing the radiation pattern may be represented by traveling waves. The traveling wave phase velocity determines the angle of peak radiation so that the TWA can be phase scanned by the adjustment of the propagation constant of the guiding structure. We can also frequency scan the TWA by taking advantage of the frequency dispersive behavior of the guiding structure. Source distributions can be synthesized to produce a prescribed radiation pattern (e.g., pencil beam, sectorial, etc), and a combination of frequency and phase scanning can be used to steer the beam. TWA design then relates the source distribution to the phase velocity and tries to implement the desired distribution in a practical structure. A large scan range is desired over a limited (e.g., 10 percent) source frequency bandwidth. The physical structure considered is a rectangular waveguide, excited by a transverse electric $(TE)_{10}$-mode (or H_{10}-mode), with a long slot in the waveguide narrow wall radiating into a half-space (i.e., an infinite flange approximation). The radiating aperture can be represented by an equivalent magnetic current quasi-line source [1, p 47].

The perturbed waveguide supports an H-type hybrid mode constructed to satisfy the required field variation as described in appendix A. The aperture admittance is obtained by the variational technique for a parallel plate waveguide radiating into a half-space as shown in appendix B. The equivalent network model includes an internal susceptance to account for the stored energy attributable to the aperture perturbation on the waveguide [2]. A transmission line description in the transverse direction is then terminated in this equivalent admittance. We use the transverse resonance technique, as described in appendix C, to determine the transverse wavenumber and thus the perturbed waveguide complex propagation constant. The slotted waveguide section then is a nonuniform, lossy transmission line in which the energy is radiated along the transmission line direction. The finite element method (FEM) is used to solve the nonuniform transmission line equations for the transmission and reflection coefficient of the slotted section from which we calculate the antenna efficiency. This network model characterizes the aperture illumination function and we obtain the radiation pattern by direct integration of the source current. The basic numerical routines to produce these calculations are included as appendix D. A thorough understanding of the radiation by this type of dispersive waveguide is required to develop a design procedure for electronically steered TWA arrays fabricated in a rectangular waveguide.

2. Leaky Wave Antenna

We consider a thin, rectangular aperture of width, d, and length, L, in a terminated rectangular waveguide having width, a, and height, b, shown in figure 1a as a leaky wave antenna structure. For narrow apertures, the waveguide perturbation is small or rather, the aperture is loosely coupled, so that the phase per unit length is slowly varying with position along the guiding structure. The leaky waveguide continuously loses energy along its length because of radiation, as shown in figure 1b. At a particular operating frequency, $f_0 = c/\lambda_0$, the main beam appears at an elevation angle, $\sin\theta_0 = (\lambda_0/\lambda_g)$, from broadside, depending on the perturbed guide wavelength, λ_g (see fig. 1a). The H_{10}-mode power available from the input waveguide, P_{inc}, is partially reflected by the slotted section with reflection coefficient, Γ_{10}. Then the input power to the TWA depends on the input impedance mismatch, $P_{\text{in}} = P_{\text{inc}} - P_{\text{reflect}} = P_{\text{inc}}(1 - |\Gamma_{10}|^2)$. We define the input efficiency, $\eta_{\text{in}} = (1 - |\Gamma_{10}|^2)$, as a measure of the power lost because of reflection, since $P_{\text{in}} = \eta_{\text{in}} P_{\text{inc}}$, is the power fed into the slotted section (see fig. 1b). The radiated power depends on the fraction of power transmitted, $|T_{10}|^2$, through the slotted section (i.e., absorbed in the matched load). If we assume that the power not transmitted is radiated, then $P_{\text{rad}} = P_{\text{in}} - P_{\text{trans}} = P_{\text{in}}(1 - |T_{10}|^2)$. Therefore, the radiation efficiency, $\eta_r = (1 - |T_{10}|^2)$, depends on the power lost in the load impedance. We group other loss mechanisms into a single absorption coefficient, A_{10}, and define an efficiency as $\eta_c = (1 - |A_{10}|^2)$. The total antenna efficiency, $\eta = \eta_{\text{in}}\eta_r\eta_c$, is a measure of the power lost because of input reflection, dissipation in the load impedance, and other losses, or $P_{\text{rad}} = \eta P_{\text{inc}}$.

For a given available power, P_{inc}, corresponding to the input power, P_{in}, in the leaky waveguide, we denote by $P(y)$ the power radiated per unit aperture length. By conservation of energy, the total power flowing at some point, $P_0(y)$, within the waveguide extending from $y_0 \equiv -L/2$ to $y = L/2$ can be written as

$$P_0(y) = P_{\text{in}} - \int_{y_0}^{y} P(\xi)d\xi \,. \tag{1}$$

Differentiating equation (1) with respect to y and defining the attenuation per unit length by

$$\alpha_r(y) = \frac{P(y)}{2P_0(y)} \,, \tag{2}$$

one finds that $P_0(y)$ must satisfy the differential equation

$$\left(\frac{d}{dy} + 2\alpha_r(y)\right) P_0(y) = 0 \,. \tag{3}$$

A wave propagating down the guide then is continuously losing energy through radiation [3]. We obtain the solution to equation (3) using the initial

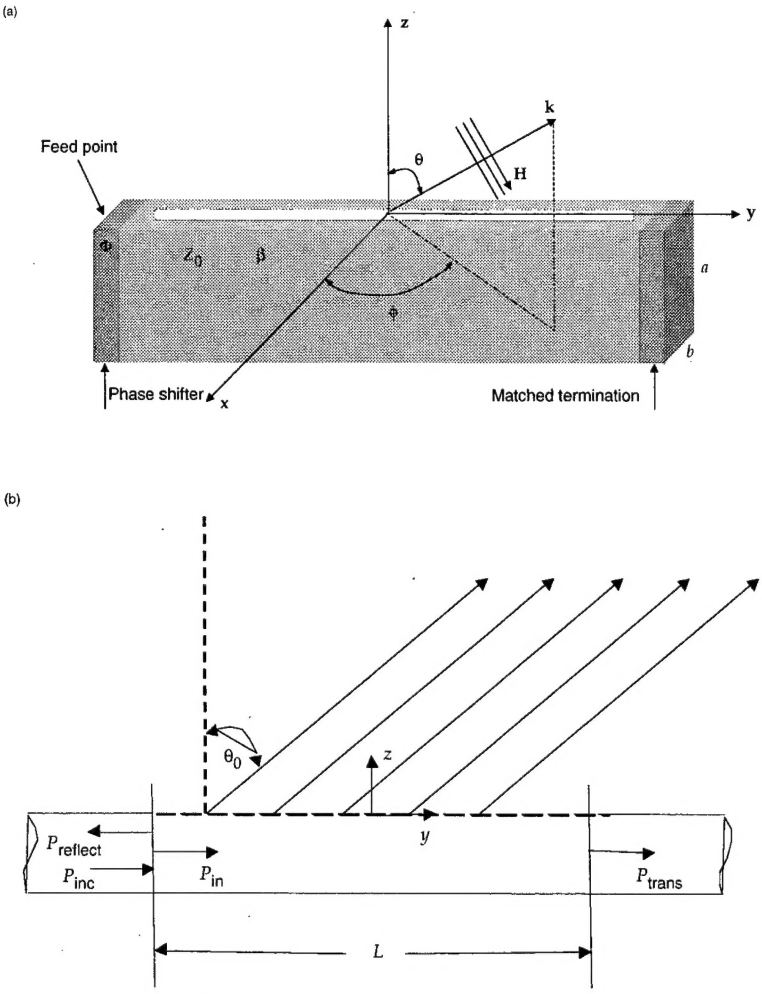

Figure 1. (a) Slotted waveguide leaky wave antenna oriented along y-axis (not to scale) and (b) general leaky wave coupling structure showing mail-beam angle.

condition, $P_{\text{in}} = P_0(y_0)$. The result is

$$P_0(y) = P_{\text{in}} \exp\left(-2\int_{y_0}^{y} \alpha_r(\xi)d\xi\right) . \tag{4}$$

Assuming no other losses (i.e., $A_{10} = 0$ or $\eta_c = 1$), the fraction of power not radiated, q, will be completely absorbed by the termination at $y = L/2$. Thus, we define

$$q \equiv \frac{P_0\left(\frac{L}{2}\right)}{P_{\text{in}}} = 1 - \frac{1}{P_{\text{in}}}\int_{y_0}^{\frac{L}{2}} P\left(\xi\right)d\xi \tag{5}$$

The radiated power per unit length is proportional to the squared magnitude of the aperture illumination function, $\mathrm{f}^2(y)$, which is proportional to the aperture electric (E-) field. That is, $P(y) = \zeta\, \mathrm{f}^2(y)$, in which ζ is a constant. Using equation (5), we find that this proportionality constant is

$$\zeta = \frac{(1-q)\,P_{\text{in}}}{\int_{y_0}^{\frac{L}{2}} \mathrm{f}^2\left(\xi\right)d\xi} \equiv \frac{\eta_r P_{\text{in}}}{I}, \quad \text{with } I \equiv \int_{y_0}^{\frac{L}{2}} \mathrm{f}^2\left(\xi\right)d\xi , \tag{6}$$

in which $\eta_r \equiv 1 - q$ is equal to the previously defined radiation efficiency. Once the magnitude of the aperture illumination function, $|\mathrm{f(y)}|$, is chosen

for the desired radiation pattern, we can calculate the required attenuation function for the leaky wave antenna by substituting $\zeta \mathrm{f}^2(y)$ into equation (2) and using equation (6) to find

$$\alpha_r(y) = \frac{\frac{1}{2}\mathrm{f}^2(y)}{\frac{1}{\eta_r} - \int_{y_0}^{y} \mathrm{f}^2(\xi)d\xi} \,. \tag{7}$$

This is an explicit solution for $\alpha_r(y)$ in terms of the aperture illumination function, which is chosen to obtain the desired radiation pattern characteristics. Then equation (7) determines the attenuation function, which is synthesized by means of an appropriate coupling structure. The fraction of power absorbed in the load can be made small but not completely zero since this would require an infinitely long antenna or an $\alpha_r(y)$ too large to be realized by physical structures.

For uniform illumination with $y_0 = -L/2$, equation (7) takes a simple form

$$\alpha_r\,(y) = \frac{\frac{1}{2}}{\frac{L}{\eta_r} - (y - y_0)} \,. \tag{8}$$

We normalize the aperture dimensions and the results to the free-space wavelength, λ_0. Using equation (8), the normalized attenuation, $|\alpha_r(y)\lambda_0|$ (in Nepers) is shown in figure 2 for $L = 20\lambda_0$, a uniform aperture illumination, and the radiation efficiency, η_r = 70, 80, and 90-percent (-1.5, -1 and -0.5 dB), as a parameter. To obtain a uniform illumination, the corresponding attenuation per unit length would require an aperture with flared width profile so that the aperture width would increase with distance toward the load. For a fixed aperture length, a larger width or flare per unit length increases the radiation efficiency but does not significantly increase the input reflection coefficient. That is, the total antenna efficiency is approximately equal to the radiation efficiency shown in figure 2.

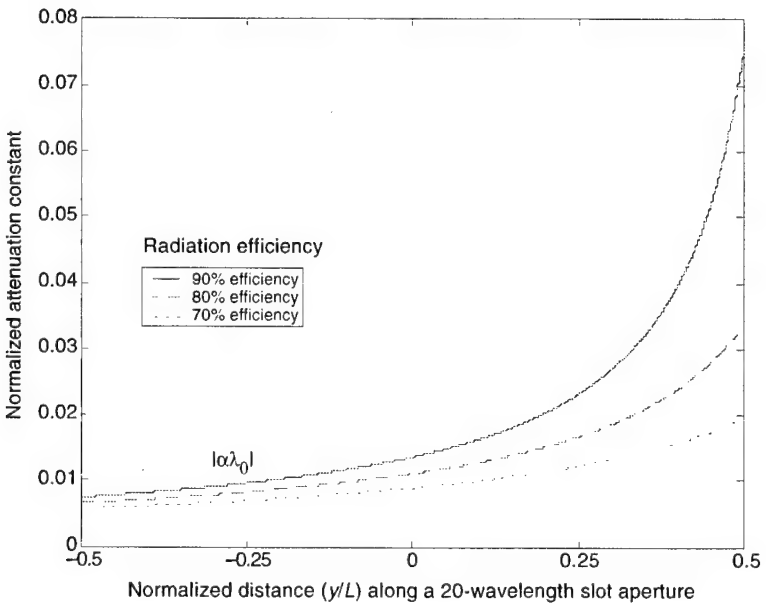

Figure 2. Normalized attenuation (in Nepers) for a uniform aperture illumination function.

Conversely, for a specified attenuation function, we can determine the aperture illumination function as follows. Define $X(y) = \mathrm{f}^2(y)$, and rewrite equation (7) as

$$\alpha_r(y) = \frac{\frac{1}{2}X(y)}{\frac{1}{\eta_r}\int_{y_0}^{\frac{L}{2}} X(\xi)d\xi - \int_{y_0}^{y} X(\xi)d\xi} \tag{9a}$$

which can be written as

$$X(y) = 2\alpha_r(y)\left\{\frac{I}{\eta_r} - \int_{y_0}^{y} X(\xi)d\xi\right\} . \tag{9b}$$

Differentiating equation (9b) with respect to y and using equation (9a) gives

$$\frac{dX(y)}{dy} = X(y)\left(\frac{d}{dy}\ln\alpha_r(y) - 2\alpha_r(y)\right) . \tag{10}$$

Solving equation (10) gives

$$X(y) = \frac{X(y_0)}{\alpha_r(y_0)}\alpha_r(y)\exp\left(-2\int_{y_0}^{y}\alpha_r(\xi)d\xi\right) . \tag{11}$$

Then in terms of $\alpha_r(y)$, the magnitude of the aperture illumination function is

$$|f(y)| = \sqrt{C\alpha_r(y)}\exp\left(-\int_{y_0}^{y}\alpha_r(\xi)d\xi\right) \tag{12}$$

in which $C = X(y_0)/\alpha_r(y_0)$ is an arbitrary constant.

For constant aperture width (normalized to waveguide height), $d = b/30$, the attenuation is calculated as developed in the next section. The corresponding normalized aperture illumination function, $\mathrm{f}(y)/\mathrm{f}(y_0)$, is shown in figure 3, which indicates that for constant aperture width, the illumination function decreases along the aperture length. The results correspond to a waveguide with $ka = 4.25$ in which $k = 2\pi/\lambda_0$ is the wavenumber. For a narrow aperture, the aperture length must be significantly increased to obtain $\eta_r > 90$ percent. For a given aperture width profile, the aperture illumination function is determined and the variation in the waveguide complex propagation constant is calculated with an equivalent network model. The basic leaky wave antenna design then simplifies to implementing the required $\alpha_r(y)$ in a slotted waveguide section. These leaky waveguide antennas can be readily combined to form a two-dimensional planar array by accounting for mutual interactions [4].

We determine the attenuation function for a section of leaky waveguide from the aperture geometry with perturbed waveguide propagation constant, $\gamma = \alpha_r + j\beta$. In general, the attenuation constant is not independent of the phase constant, but the waveguide cross section can be adjusted to keep $\beta = 2\pi/\lambda_g$ approximately constant while α_r [2, p 190] is varied. Radiating elements fabricated in the waveguide narrow wall allow the use of specialized waveguide types such as dielectric loaded or ridged waveguide, which provide additional design flexibility. Typical examples are shown in

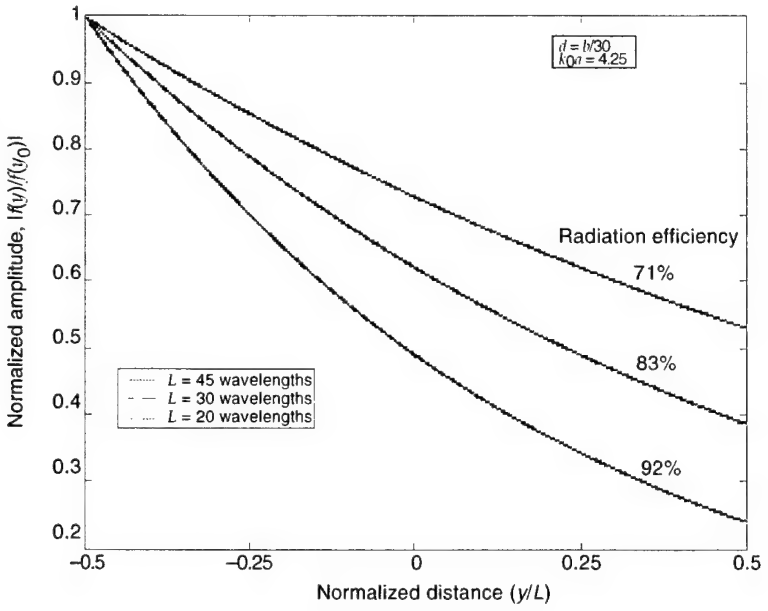

Figure 3. Aperture illumination function for a constant width aperture with radiation efficiency as a parameter.

figure 4a for radiating elements in the narrow wall of a rectangular waveguide [1, p 282]. We have investigated tapered and flared transition sections as shown in figure 4b as a "discontinuity minimizer" to avoid exciting higher order modes [1, p 284].

As an example, we consider an aperture with a constant width section, $d_0 = b/40$, and total length (normalized to waveguide width), $L = 30a$. We include either a tapered input section or a flared output section of length $L_1 = L/2$ and $L_2 = L/2$, respectively. For narrow apertures, the input reflection is small with $\eta_{\text{in}} > 97$-percent (-0.1 dB). Nevertheless, the phase variation over the tapered section produced an antenna pattern with increased side lobe level (SLL). Although not described in detail, the results for variable aperture width demonstrated that tapered or flared sections (see fig. 4b) are undesirable in terms of SLL. A flared output section provides a better approximation to a uniform aperture illumination, as can be surmised from equation (12). However, the flared (or tapered) aperture width corrupts the radiation pattern, as shown in figure 5. The tapered input distorts the SLL below the main beam angle, θ_0 (i.e., in the forward direction), while a flared output affects the SLL above θ_0 (i.e., toward broadside). By sacrificing efficiency (or increasing the aperture length), one can make the taper (or flare) more gradual to improve the pattern characteristics. This would be undesirable for most practical TWA structures, so we consider only constant width apertures. Parametric studies of leaky wave guides with constant aperture width are presented to develop a complete design procedure for this type of antenna.

Figure 4. (a) Perturbed waveguide antenna examples: TE long slot and holey rectangular waveguide showing tapered transition sections, and (b) an aperture with a constant width section and either a tapered input or a flared output section.

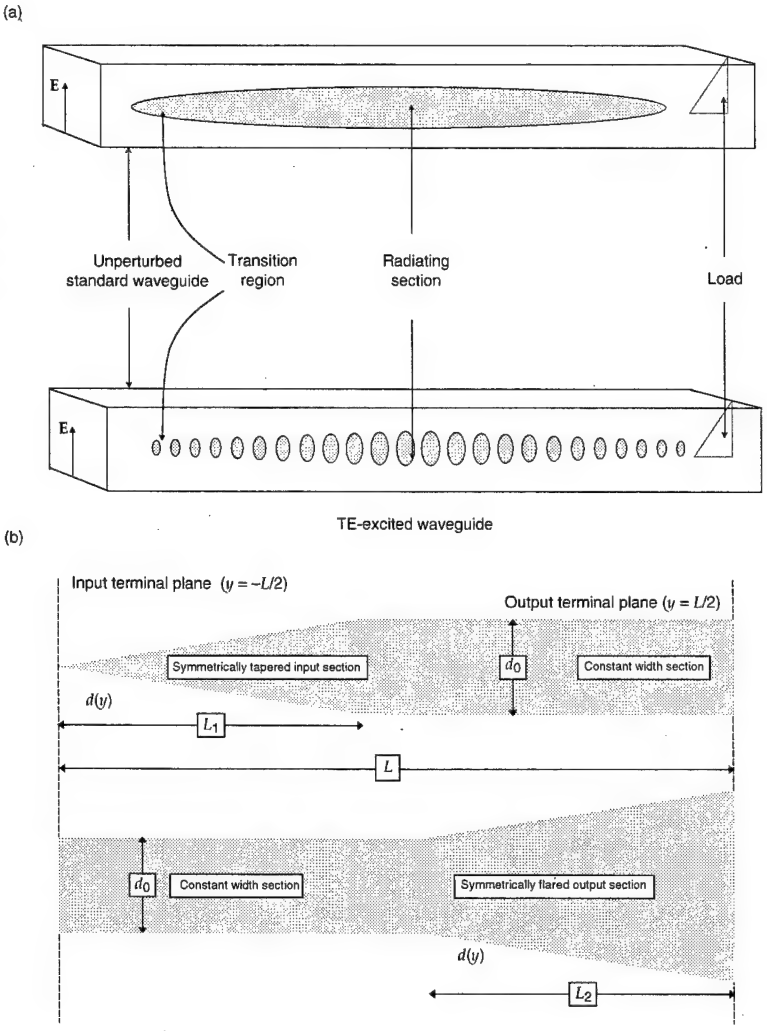

Figure 5. Radiation pattern of a leaky waveguide having an aperture with tapered input or flared output sections.

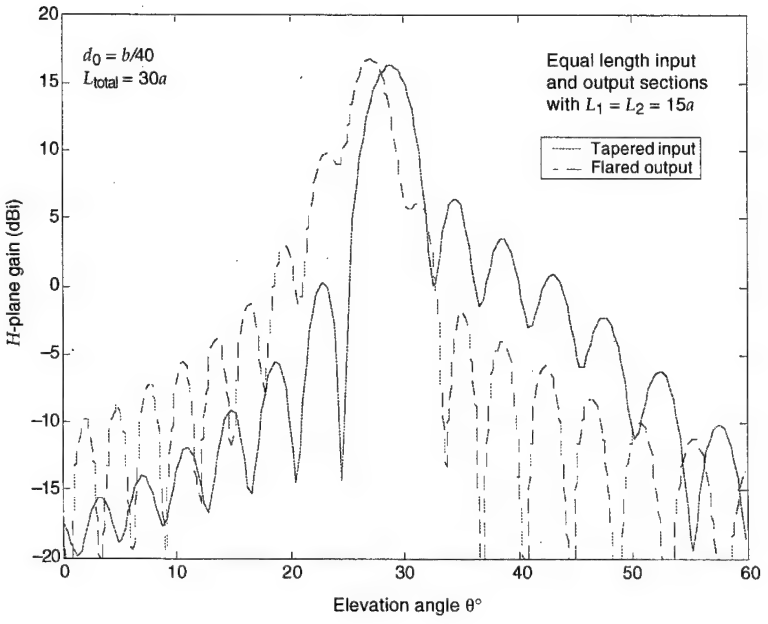

3. Perturbation Solution

Consider an aperture fed by a parallel plate waveguide radiating into a half-space (i.e., an infinite flange approximation), as shown in figure 6, where the origin is centered in the aperture. We consider radiation into a half-space rather than free space in anticipation of constructing an antenna array of leaky waveguides. In the direction transverse to the propagation direction y, the medium parameters over each waveguide cross section are constant so that a modal decomposition is possible. However, the waveguide fields in the presence of the aperture cannot be described by a single TE or transverse magnetic (TM)-mode. We construct an alternate modal decomposition to have the correct spatial variation and satisfy the boundary conditions. Following the analysis of Goldstone and Oliner [5], the result is a predominantly TE- or H-type mode, as shown in appendix A. For now, consider an air-filled waveguide having free-space permittivity, $\epsilon = \epsilon_0$ and permeability, $\mu = \mu_0$, propagating time-harmonic electromagnetic (EM) fields with the time dependence, $e^{j\omega t}$ suppressed. Since there is no variation of the waveguide in the direction of propagation, the wavenumber in this direction is the same for all modes or $k_{yn} = \beta_n = \beta$. $k_{t0} = k_{z0} = \sqrt{k^2 - \beta^2}$ is the wavenumber in the transverse (to y) direction, and $Z_{H0} = \omega\mu_0/k_{z0}$ is the H-type mode characteristic (wave) impedance. We develop a composite equivalent circuit to approximate the aperture of infinite length as shown in appendix B. We use the transverse resonance method described in appendix C to determine the transverse wavenumber for the transverse transmission line terminated in this equivalent circuit.

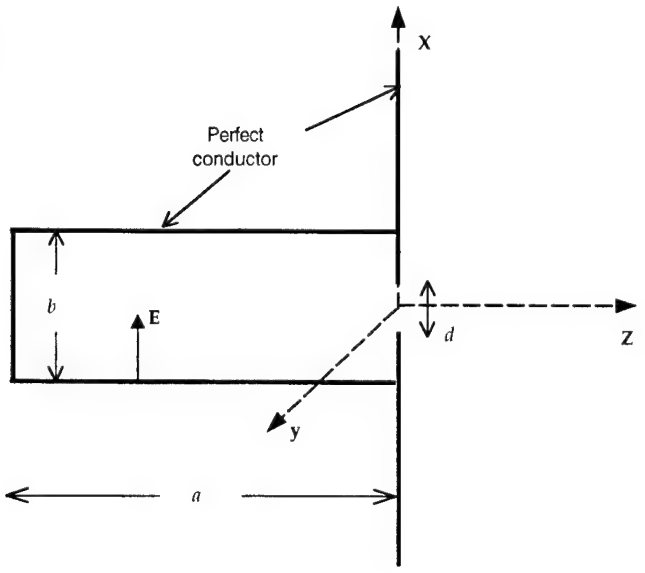

Figure 6. A rectangular waveguide-fed aperture radiating into a half-space.

The transverse resonance solution provides the perturbed waveguide phase constant with the leaky wave attenuation function (see sect. 2) to completely characterize the aperture source so that antenna gain can be calculated. We then extend the result to the finite length aperture by using the FEM to calculate the aperture radiation efficiency (see app D).

3.1 Parallel Plate Fed Aperture

A parallel plate transverse electromagnetic (TEM)-mode polarized along x is incident on an infinitely long aperture of constant width radiating into a half-space as shown in figure 7. In appendix A, we develop an alternate modal decomposition that can represent the aperture perturbation on the waveguide fields for H-mode or TE-excitation. In appendix B, we show that energy propagation in the parallel plate region is equivalent to an obliquely incident TEM wave on the aperture plane. An H-type modal decomposition is used when the TEM fields are the modal fields transverse to the direction of incidence (see fig. B-2). We derive a variational expression, equation (B-38) for the radiation admittance of the parallel plate waveguide by assuming a constant aperture field. We then extend this expression to the case of a narrow aperture (i.e., when the aperture width is not the full waveguide height). The variational expression is normalized to the characteristic admittance of the propagating wave, which for an incident H_{10}-mode is that of the fundamental H-type mode, so from equation (A-16),

$$Y_{H0} = \frac{1}{Z_{H0}} = \frac{k_{z0}}{\omega \mu_0} . \tag{13}$$

Figure 7. A parallel plate waveguide radiating into a half-space.

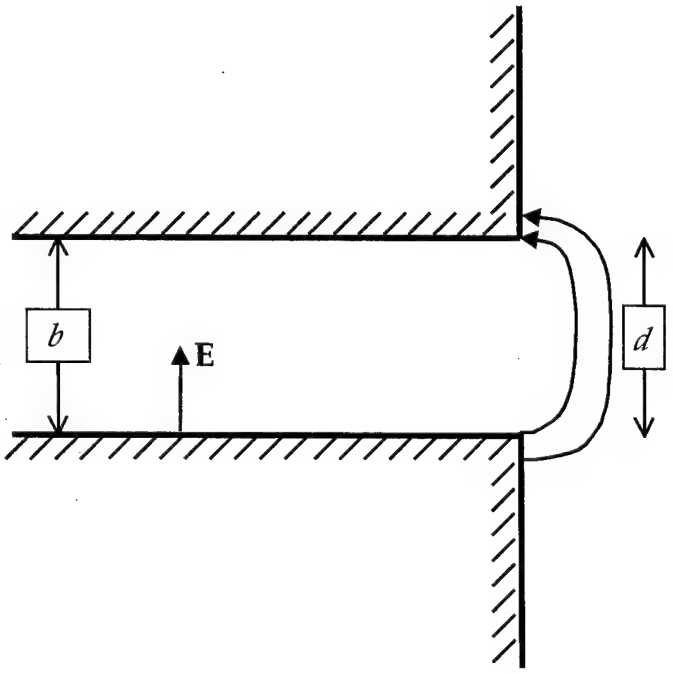

The variational result equation (B-29) derived in appendix B depends on the E-field in the aperture. For a constant aperture field, one obtains the approximation equation (B-30) to the variational expression. This result was obtained by Marcuvitz using the variational method [3] and includes only the susceptance outside the aperture, because it depends only on the external E-field. Then under the same assumptions, equation (B-30) provides the external admittance of a narrow aperture by replacing b with d. This is because the power per unit length radiated by the aperture is independent of the height of the feeding waveguide, as long as the aperture field is unchanged [1]. For a constant aperture E-field, the normalized input admittance of a parallel plate fed aperture of width $d < b$ is from appendix B:

$$y_{\text{in}}^{\text{ext}} \equiv \frac{Y_{\text{in}}}{Y_{H0}} = \int_0^{k_{z0}d} H_0^{(2)}(\xi)d\xi - H_1^{(2)}(k_{z0}d) + \frac{2j}{\pi k_{z0}d} = \frac{G^{\text{ext}}}{Y_{H0}} + j\frac{B^{\text{ext}}}{Y_{H0}}, \tag{14}$$

in which $H_\nu^{(2)}$ is the Hankel function of the second kind, order ν. We use the small argument form of the cylindrical Bessel functions [8, p 935] in equation (B-38) to obtain a closed form approximation to the external conductance and susceptance [3, p 184]

$$\frac{G^{\text{ext}}}{Y_{H0}} = \frac{k_{z0}d}{2}, \quad \text{and} \tag{15}$$

$$\frac{B^{\text{ext}}}{Y_{H0}} = \frac{k_{z0}d}{\pi}\ln\left[\frac{\pi e}{g k_{z0}d}\right]. \tag{16}$$

The irrational number, e = 2.71828..., is the base of the natural logarithm and $g = e^c = 1.781...$, in which the irrational number $c = 0.577...$, is Euler's constant. This represents the "external" equivalent circuit parameters of a waveguide-fed, narrow aperture radiating into a half-space.

We obtain the "internal" circuit by considering the aperture as a symmetrical capacitive iris oriented along the y-axis, as shown in figure 8a. The internal fringing field of the aperture is accounted for by the internal susceptance of this symmetrical, zero-thickness "window." The approach is to

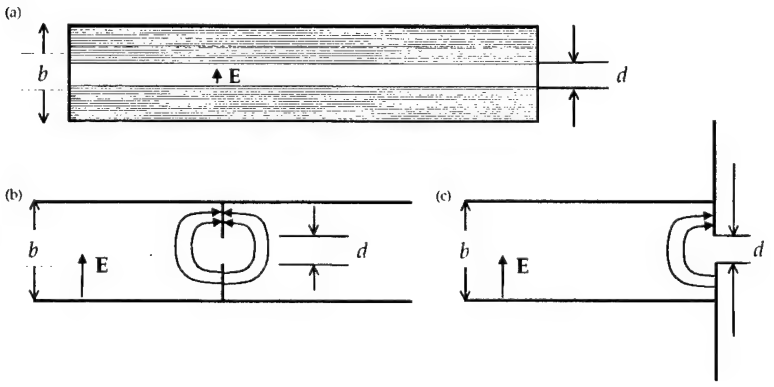

Figure 8. A composite circuit model for parallel plate fed aperture developed by analog to a capacitive iris: (a) a symmetrical, capacitive iris in rectangular waveguide, a cross-sectional view, (b) fringing field of an iris, side view, and (c) internal fringing field of a parallel plate fed aperture.

consider the fringing fields on each side of the perforated surface as indicated schematically in figure 8b. The equivalent circuit parameters for a zero-thickness window are obtained by the equivalent static method for a static aperture field attributable to incidence of the two lowest H-modes [2, p 219]. The result is the capacitive susceptance given in equation (2a) of *The Waveguide Handbook*, in terms of the guide wavelength in the direction of propagation [2]. For our case of a narrow aperture, we have $d \ll b$, so in this expression, the second term reduces to the function Q_2 and the last term vanishes. Furthermore, the waveguide height is small compared to wavelength, or $b \ll \lambda_g$ so that $Q_2 \sim 0$ and the second term is negligible. Then for the transverse transmission line with guide wavelength, λ_{gz}, the normalized iris susceptance is the leading term of equation (2a) [2, p 218]

$$\frac{B_{\text{iris}}}{Y_{H0}} = \frac{4b}{\lambda_{gz}} \ln\left[\csc\left(\frac{\pi d}{2b}\right)\right], \quad \lambda_{gz} = \frac{2\pi}{k_{z0}}. \tag{17}$$

By symmetry, we use one-half of this result for the iris in the closed waveguide to represent the internal susceptance of the aperture as indicated in figure 8c.

The internal susceptance for the waveguide fed aperture is then

$$\frac{B^{\text{int}}}{Y_{H0}} = \frac{k_{z0}b}{\pi} \ln\left[\csc\left(\frac{\pi d}{2b}\right)\right], \tag{18}$$

reducing to a short circuit when $d = 0$. We combine the admittance inside and outside the waveguide to obtain a composite equivalent circuit for a transverse resonance analysis. The circuit parameters are the combination of equations (15), (16), and (17), or

$$\frac{G}{Y_{H0}} = \frac{G^{\text{ext}}}{Y_{H0}} = \frac{k_{z0}d}{2}, \quad \text{and} \tag{19}$$

$$\frac{B}{Y_{H0}} = \frac{B^{\text{ext}}}{Y_{H0}} + \frac{B^{\text{int}}}{Y_{H0}} = \frac{k_{z0}d}{\pi} \ln\left[\frac{\pi e}{g k_{z0} d}\right] + \frac{k_{z0}b}{\pi} \ln\left[\csc\left(\frac{\pi d}{2b}\right)\right]. \tag{20}$$

The aperture admittance for this composite equivalent circuit model, $Y_A(k_{z0}) = G + jB$, then depends on the transverse wavenumber and the aperture geometry. This approximation is only appropriate for the idealized case of zero wall thickness and an infinite waveguide flange but provides useful results for narrow apertures. A refined equivalent circuit to account for the waveguide wall thickness could be developed but is not required at this point to obtain engineering results. However, the equivalent circuit must be modified for an array of such leaky waveguide antennas, including mutual interactions between nearby radiating elements [4].

The cross section of the physical structure shown in figure 9a is analyzed with the transverse resonance technique that is described in appendix C. We use the network representation shown in figure 9b to terminate the transverse transmission line that propagates the fundamental H-type mode. A transverse field modal decomposition in terms of rectangular

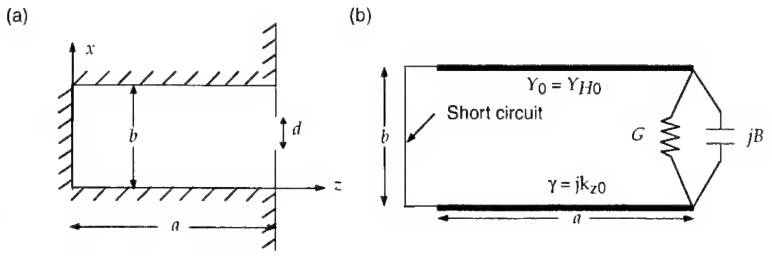

Figure 9. An infinitely long aperture in the narrow wall of rectangular waveguide radiating into a half-space: (a) a waveguide-fed aperture and (b) equivalent circuit model for transverse transmission line.

waveguide TE- and TM-modes would require a transmission line representation for each mode that is then coupled by the aperture. An advantage of the H-type modal representation is that the transverse transmission line consists of one transmission line of characteristic admittance Y_{H0}, and propagation constant jk_{z0}. This transmission line is shorted at one end and terminated in a lumped admittance at the other end. The transverse resonance condition requires that at resonance, the input admittance "looking" in each direction must sum to zero at any point along the line. We use the coordinate system shown in figure 9a, so for any point $0 \leq z' \leq a$ we have

$$\overleftarrow{Y}_{\text{in}}(z') + \vec{Y}_{\text{in}}(z') = 0\,, \tag{21}$$

in which the arrows denote the input admittance looking to the left or right, respectively [7, p 167].

At the aperture plane ($z' = a$), the admittance looking to the right is Y_A while that to the left corresponds to a short circuit located a distance "a" down the line (i.e., at $z' = 0$). The resulting network resonance equation at this terminal plane is then [2, p 10]

$$-j\cot(k_{z0}a) + \frac{G}{Y_{H0}} + j\frac{B}{Y_{H0}} = 0\,, \tag{22}$$

which generally requires numerical solution. An approximate analysis is obtained by the perturbation method since the leaky waveguide propagation constant can be regarded as a perturbation on the propagation constant of modes in the closed waveguide. This approach provides an analytical approximation for the transverse wavenumber as opposed to a numerical evaluation of equation (22). The result is an analytical approximation to the perturbed fundamental mode propagation constant, $\gamma_0 = j\beta$, which is useful in the study of leaky wave antennas.

The analysis assumes that the aperture perturbs the transverse wavenumber from its value in the closed guide. Then for H_{10}-mode propagation, the transverse wavenumber is not much different than $\kappa = \pi/a$—the unperturbed wavenumber of the lowest mode. Then for a small perturbation, the left side of equation (22) is approximated by two terms in a Taylor series expansion $\overleftarrow{Y}(k) = \overleftarrow{Y}(k_{z0}) + \vec{Y}(k_{z0})$, at some frequency corresponding to

the wavenumber, k. Then with $\Delta k_{z0} = k_{z0} - \kappa$, we can write

$$\vec{Y}(k) = \vec{Y}(\kappa) + \left.\frac{d\vec{Y}\,(k_{z0})}{dk_{z0}}\right|_{k_{z0}=\kappa} \Delta k_{z0} \approx 0\,, \tag{23}$$

since for a small perturbation equation (22) will nearly vanish at resonance. Substituting equation (22) evaluated at κ into equation (23), we have

$$\Delta k_{z0} = -\frac{\vec{Y}(\kappa)}{\left.\frac{d\vec{Y}(k_{z0})}{dk_{z0}}\right|_{k_{z0}=\kappa}} = -\frac{-j\cot(\kappa a) + \vec{Y}(\kappa)}{aj\csc^2(\kappa a) + \left.\frac{d\vec{Y}(k_{z0})}{dk_{z0}}\right|_{k_{z0}=\kappa}} \approx \frac{j}{a}\frac{\vec{Y}(\kappa) - j\cot(\kappa a)}{\csc^2(\kappa a)}\,. \tag{24}$$

The approximation is valid over a wide range since the derivative term is inversely proportional to the fourth power of the admittance magnitude and so is neglected. With the same argument, the equivalent expression in terms of impedance quantities is

$$\Delta k_{z0} \approx \frac{j}{a}\frac{\vec{Z}(\kappa) + j\tan(\kappa a)}{\sec^2(\kappa a)}\,. \tag{25}$$

For a narrow aperture (i.e., $d/b \ll 1$), we take the first approximation to k_{z0} as κ corresponding to the unperturbed waveguide propagating the H_{10}-mode. Then with $\kappa = \pi/a$, the perturbation to the transverse wavenumber, Δk_{z0}, is calculated. The approximate result for such a perturbation about a short circuit (i.e., the closed waveguide) is then

$$\Delta k_{z0} = \frac{j}{a}\vec{Z} = \frac{j}{a}\left.\left(\frac{G - jB}{G^2 + B^2}\right)\right|_{k_{z0}=\kappa} = \frac{B'}{a(G'^2 + B'^2)} + \frac{j}{a}\frac{G'}{(G'^2 + B'^2)} \tag{26}$$

in which the equivalent circuit parameters are evaluated at $k_{z0} = \kappa = \pi/a$, or

$$G' \equiv G(\kappa) = \frac{\pi d}{2a} \quad \text{and} \quad B' \equiv B(\kappa) = \frac{b}{a}\ln\left[\csc\left(\frac{\pi d}{2b}\right)\right] + \frac{d}{a}\ln\left[\frac{ae}{gd}\right]\,. \tag{27}$$

The fundamental mode transverse wavenumber is then

$$k_{z0} = \kappa + \Delta k_{z0} = \frac{\pi}{a} + \frac{B'}{a\,(G'^2 + B'^2)} + \frac{j}{a}\frac{G'}{(G'^2 + B'^2)}\,. \tag{28}$$

The complex propagation constant of the fundamental mode, $\gamma_0 = \sqrt{k^2 - k_{z0}^2} = \alpha_r + j\beta$, can then be calculated with the root chosen so that the attenuation is negative ($\alpha_r < 0$) for propagation in the positive y-direction, or $\beta = k_{y0}$. The propagation constant reduces to that of the closed waveguide when $d = 0$ since the equivalent network becomes a short circuit. Note that the result often found in the literature for leaky wave structures of this type [1, p 189] involves another approximation not used here. The propagation constant is often approximated by a binomial expansion with higher order terms neglected, or

$$\frac{\gamma_0}{k} = \sqrt{1 - \left(\frac{k_{z0}}{k}\right)^2} \approx 1 - \frac{1}{2}\left(\frac{k_{z0}}{k}\right)^2 + O\left(k_{z0}^4\right) . \tag{29}$$

This approximation holds when the operating frequency is well above the cutoff frequency of the unperturbed mode [5] and so does not provide the correct behavior at low frequency. We prefer to calculate the complex propagation constant from equation (29) without approximation since operation near cutoff is often of practical interest.

3.2 Aperture in a Rectangular Waveguide

Now that γ_0 for the parallel plate fed aperture can be calculated with sufficient accuracy as a function of f_0, consider the finite length aperture in a rectangular waveguide. We assume that the waveguide width is sufficient to allow the parallel plate guide analysis to apply to the rectangular waveguide. This requires that higher order modes associated with the aperture perturbation be rapidly attenuated so that a single propagating mode can be used in the transverse resonance analysis. Such a leaky waveguide supports H-type hybrid modes constructed to have the required spatial variation (see app A). The approach is to allow for a longitudinal variation in $d(y)$ and thus variable $\gamma_0(y)$ over the total aperture length, L. The input and output air-filled waveguide propagates a single H_{10}-mode with propagation constant $\beta = \beta_{10} = \sqrt{k_0^2 - \left(\frac{\pi}{a}\right)^2}$ for the fundamental $(m = 1, n = 0)$ mode. The H_{10}-mode characteristic impedance is $Z_{10} = \frac{\omega\mu_0}{\beta_{10}}$, but when perturbed by the aperture, the characteristic impedance becomes that of the H-type fundamental mode, $Z_{H0} = \frac{\omega\mu_0}{k_{z0}}$. This leads to a nonuniform transmission line representation along the aperture length

$$-\frac{d}{dy}V(y) = j\gamma_0(y)Z_{H0}I(y) \quad \text{and} \quad -\frac{d}{dy}I(y) = j\gamma_0(y)Y_{H0}V(y) , \tag{30}$$

which is solved numerically with the FEM with linear interpolation functions [8, p 33]. The H-type mode impedance variation with y is neglected since for the fundamental mode

$$\frac{d}{dy}Z_{H0}(y) = \frac{d}{dy}\frac{\omega\mu_0}{k_{z0}(y)} = -\frac{\omega\mu_0}{k_{z0}^2(y)}\frac{d}{dy}k_{z0}(y) \approx 0 , \tag{31}$$

because $\mathrm{Re}(k_{z0}(y)) > 0$ is a slowly varying function of position. Then the transmission line voltage (and current) satisfies the differential equation

$$-\frac{d}{dy}\left(\varsigma(y)\frac{d}{dy}V(y)\right) + \zeta(y)V(y) = 0 , \tag{32}$$

in which $\varsigma(y) = -((\gamma_0(y)Z_{H0}(y))^{-1}$, and $\zeta(y) = \gamma_0(y)/Z_{H0}(y)$. The distributed discontinuity attributable to the (possibly variable) aperture width, $d(y)$, then causes a reflection in the input waveguide, as indicated in figure 10, where now the aperture extends from $y = 0$ to $y = L$. For constant aperture width, the H-type fundamental mode impedance is constant. However, there is an impedance mismatch at the terminal planes

Figure 10. H_{10}-mode incident on a leaky waveguide section with matched termination.

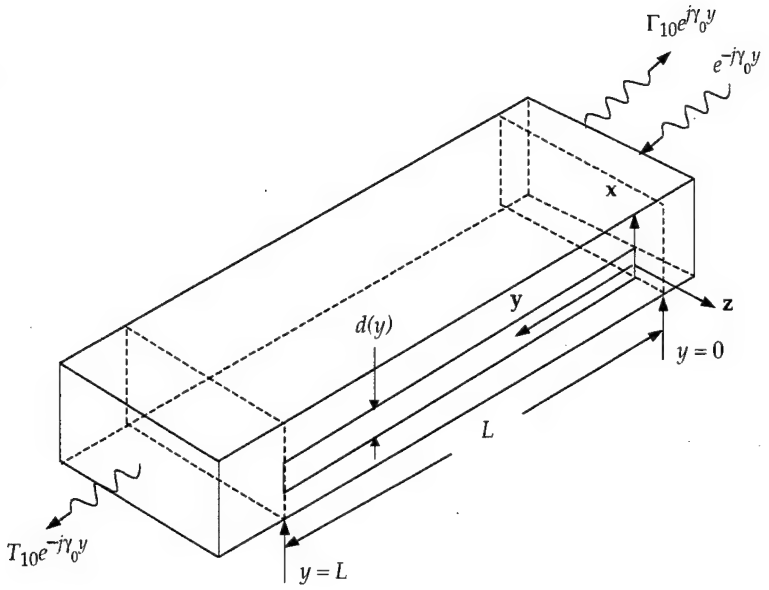

where the transmission line impedance is Z_{10} so that $Z_{H0}(0) = Z_{H0}(L) = Z_{10}$. Transmission to the matched output waveguide is also obtained in the FEM solution with the remaining power radiated by the aperture. For a single incident mode with unit input voltage, the total voltage for $y < 0$ is then

$$V(y) = e^{-j\gamma_0 y} + \Gamma_{10} e^{j\gamma_0 y} , \tag{33}$$

in which Γ_{10} is the voltage reflection coefficient at the input terminal plane of a finite length section of leaky waveguide. The boundary conditions at the terminal planes are determined from the functional for the differential operator in equation (32) [8, p 34]. Minimizing the functional establishes the matrix equation to solve where the boundary terms can be cast in the form of boundary conditions of the third kind (or mixed boundary conditions). However, the derivative terms at the boundary $y = 0$ are taken in the negative sense so that in general, boundary condition is written as $\pm\varsigma(dV/dy) + \chi V = \rho$. The negative sign is used at $y = 0$ so

$$-\varsigma \frac{dV}{dy}\bigg|_{y=0} = \frac{-j\gamma_0}{\gamma_0 Z_{H0}(y)} \left(e^{-j\gamma_0 y} - \Gamma_{10} e^{j\gamma_0 y}\right)\bigg|_{y=0} = -\frac{j}{Z_{H0}(y)} \left(e^{-j\gamma_0 y} - \Gamma_{10} e^{j\gamma_0 y}\right)\bigg|_{y=0} , \tag{34a}$$

and we can identify

$$\chi_0 = -\frac{j}{Z_{10}} \quad \text{and} \quad \rho_0 = -\frac{2j}{Z_{10}} . \tag{34b}$$

The subscript denotes the input terminal plane at $y = 0$ where $Z_{H0}(0) = Z_{10}$. Similarly, for $y > L$, the voltage is $V(y) = T_{10} e^{-j\gamma_0 y}$ in which T_{10} is the slotted waveguide transmission coefficient. Then at $y = L$, we have

$$\varsigma \left.\frac{dV}{dy}\right|_{y=L} = \frac{-j\gamma_0}{-\gamma_0 Z_{H0}(y)} \left(\mathrm{T}_{10} e^{-j\gamma_0 y}\right)\Big|_{y=L} = \frac{j}{Z_{H0}(y)} \mathrm{T}_{10} e^{-j\gamma_0 y}\Big|_{y=L} . \tag{35a}$$

Thus, we can identify

$$\chi_L = -\frac{j}{Z_{10}} \quad \text{and} \quad \rho_{L=0} \tag{35b}$$

at the end of the finite length aperture where $Z_{H0}(L) = Z_{10}$. The transmission line voltage, $V(y)$ is obtained directly from the FEM solution once $\gamma_0(y)$ is input from the transverse resonance result for a given aperture width profile, $d(y)$. The distributed impedance discontinuity in the leaky waveguide section reflects some power to the input waveguide and transmits some power to the output waveguide assumed to be terminated in a matched load (or infinite in extent).

The transmission line model characterizes propagation on a nonuniform, lossy transmission line by the variation in $\gamma_0(y)$ over the length of the waveguide section (for variable $d(y)$). The power lost because of dissipation in the leaky waveguide is considered completely radiated. At $y = 0$, the voltage is given by equation (33) so that $\gamma_{10} = V(0) - 1$. At $y = L$, $V(L) = T_{10} e^{-j\gamma_0(L)L}$ with $\gamma_0(L) = \gamma_0(0) = \beta_{10}$ at each end of the leaky waveguide section. The reflection and transmission coefficients are determined from the FEM voltage solution. We define the antenna efficiency as the combination of the input efficiency (reflection loss), the radiation efficiency (load dissipation) and other losses combined into η_c (typically dominated by conductor losses)

$$\eta = \eta_{\mathrm{in}} \eta_r \eta_c = \left(1 - |\Gamma_{10}|^2\right) \left(1 - |\mathrm{T}_{10}|^2\right) \left(1 - |\mathrm{A}_{10}|^2\right) \tag{36}$$

with the absorption coefficient, A_{10}, presently neglected or $\eta_c = 1$. We investigated the convergence of the FEM solution by increasing the number of cells used per guide wavelength. The results showed that a FEM mesh with more than 75 cells per guide wavelength is required for the solution to converge. For the results presented, we used an FEM mesh with 100 cells per guide wavelength to calculate η (see app D). A tapered transition region to the constant width section does reduce Γ_{10}, but the effect is insignificant for a narrow aperture. For the finite length apertures considered, the effect of tapered input and output transition sections on Γ_{10} is negligible but can distort the radiation pattern as previously mentioned.

4. Radiation Pattern

The radiated fields produced by arbitrary current distributions can be calculated with the appropriate Green's function, which is the radiated field of an infinitesimal source [8, p 909]. For a rectangular aperture symmetrically located in the coordinate system of figure 6 (also see fig. 1), the far fields in free space are computed with

$$\mathbf{E}(\mathbf{r}) \approx \left\{ \begin{array}{l} \frac{-jk}{4\pi r} e^{-jkr} \times \\ \int_{y_0}^{\frac{L}{2}} \int_{-\frac{d}{2}}^{\frac{d}{2}} (\cos\theta \sin\phi \hat{\mathbf{p}} - \cos\phi \hat{\mathbf{t}}) E_x(x', y') e^{j(k \sin\theta \sin\phi - \beta(y'))y'} e^{jk \sin\theta \cos\phi x'} dx' dy' \end{array} \right\}, \quad \text{and} \tag{37a}$$

$$\mathbf{H}(\mathbf{r}) \approx \left\{ \begin{array}{l} \frac{-j\omega\varepsilon_0}{4\pi r} e^{-jkr} \times \\ \int_{y_0}^{\frac{L}{2}} \int_{-\frac{d}{2}}^{\frac{d}{2}} (\cos\theta \sin\phi \hat{\mathbf{t}} + \cos\phi \hat{\mathbf{p}}) E_x(x', y') e^{j(k \sin\theta \sin\phi - \beta(y'))y'} e^{jk \sin\theta \cos\phi x'} dx' dy' \end{array} \right\} \tag{37b}$$

where $\hat{\mathbf{t}}$ and $\hat{\mathbf{p}}$ are unit vectors in the θ and ϕ directions, respectively. Here $E_x(x', y')$ is the aperture E-field and $\beta(y')$ is the perturbed waveguide phase constant at each position y'. In the far zone, the EM fields are of the form

$$\mathbf{E}(\mathbf{r}) \approx \frac{e^{-jkr}}{r} \sqrt{\xi_0} \mathbf{F}(\theta, \phi) \times \hat{\mathbf{r}} \quad \text{and} \quad \mathbf{H}(\mathbf{r}) \approx \frac{e^{-jkr}}{r} \sqrt{\eta_0} \mathbf{F}(\theta, \phi), \tag{38}$$

in which $\xi_0 = 120\pi$-ohm is the free-space impedance and $\eta_0 = 1/\xi_0$ is the free-space admittance. The average power radiated per unit area is then

$$\mathbf{S} = \mathbf{E} \times \mathbf{H}^* = \frac{(\mathbf{F} \times \hat{\mathbf{r}})^* \times \mathbf{F}}{r^2} = \hat{\mathbf{r}} \frac{|\mathbf{F}(\theta, \phi)|^2}{r^2}, \tag{39}$$

so $|\mathbf{F}(\theta\phi)|^2$ is the average power radiated per steradian. The directive gain is the radiated power per steradian normalized to the total radiated power,

$$P_{\text{total}} = \iint_{4\pi} |\mathbf{F}(\Omega)|^2 d\Omega = \int_0^{2\pi} \int_0^{\pi} |\mathbf{F}(\theta, \phi)|^2 \sin\theta \, d\theta \, d\phi \tag{40}$$

averaged over all solid angles (i.e., 4π steradian). Therefore, the directivity (or directive gain) is given by

$$G(\theta, \phi) = \frac{4\pi |F(\theta, \phi)^2|}{P_{\text{total}}} \tag{41}$$

in dB relative to an isotropic radiator (dBi) and is independent of amplitude scale factors. The realized gain (or simply gain) includes the antenna efficiency as calculated with the FEM (see sect. 3.2). The realized gain, $G_r(\theta, \phi)$,

includes losses such as the input impedance mismatch (η_{in}), the power dissipated in the load (η_r), and other possible loss mechanisms such as conductor or dielectric loss (η_c). The calculated results are presented as realized gain, based on the total antenna efficiency, or $G_r(\theta, \phi) = \eta G(\theta, \phi)$.

The finite width rectangular aperture can be represented by an equivalent rectangular sheet of current extending from $x = -d/2$ to $x = d/2$ and $y = -L/2$ to $y = L/2$ (see fig. 1a). Since there are no transverse currents excited for the assumed aperture E-field, the amplitude depends only on axial position, $E_x(x', y') = E_x(y')$. Then even for variable aperture width, $d(y')$, the integral in equation (37) along the x-direction simplifies to

$$\int_{-\frac{d(y')}{2}}^{\frac{d(y')}{2}} E_x(x', y') e^{jk \sin\theta \cos\phi x'} dx' = E_x(y') \int_{-\frac{d(y')}{2}}^{\frac{d(y')}{2}} e^{jk \sin\theta \cos\phi x'} dx' = E_x(y') \frac{\sin(u_x(y'))}{u_x(y')} , \qquad (42)$$

in which $u_x(y') = \pi d(y') \sin\theta \cos\phi / \lambda_0$. However, we only consider narrow apertures in which $d(y') \ll \lambda_0/2$ so $u_x(y') = u_x \ll 1$ and the aperture field in equation (37) reduces to a magnetic current line source as shown in figure 11 where

$$\mathbf{M} = -\hat{\mathbf{z}} \times \mathbf{E} = -E_x(y')\hat{\mathbf{y}} . \qquad (43)$$

Then in equation (42), the radiation pattern is not modified by the finite aperture width as long as it is small compared to wavelength (i.e., $d < \lambda_0/2$) [1, p 47].

For constant aperture width, $u_x(y') = u_x = \pi d \sin\theta \cos\phi / \lambda_0$, and $E_x(x', y') = E_x(y')$ The line source amplitude is the aperture illumination function magnitude from equation (12), or

$$E_x(y') \equiv |\mathrm{f}(y')| \int_{-\frac{d}{2}}^{\frac{d}{2}} e^{jk \sin\theta \cos\phi x'} dx' = |\mathrm{f}(y')| \frac{\sin u_x}{u_x} \cong |\mathrm{f}(y')| \qquad (44)$$

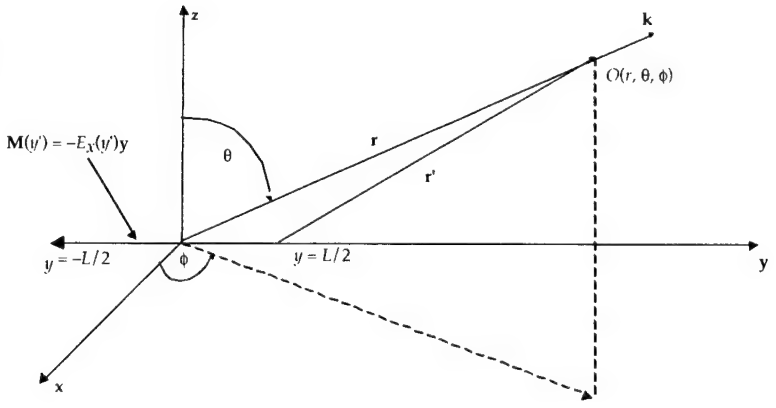

Figure 11. A narrow aperture represented by a magnetic current line source in spherical coordinates.

This aperture field has the phase variation of the perturbed waveguide phase constant which is now independent of position in the aperture, $\beta(y') = \beta$. Here, we consider constant width apertures so that results for variable aperture width are shown only in figure 5. For the narrow widths of interest, the far fields in the upper half-space are from equation (37)

$$\mathbf{E}(\mathbf{r}) \approx \left\{ \frac{jk}{2\pi r} e^{-jkr} \int_{y_0}^{\frac{L}{2}} (\cos\theta \sin\phi \hat{\mathbf{p}} - \cos\phi \hat{\mathbf{t}}) E_x(y') e^{j(k \sin\theta \sin\phi - \beta)y'} dy' \right\}, \quad \text{and} \tag{45a}$$

$$\mathbf{H}(\mathbf{r}) \approx \left\{ \frac{j\omega\varepsilon_0}{2\pi r} e^{-jkr} \int_{y_0}^{\frac{L}{2}} (\cos\theta \sin\phi \hat{\mathbf{t}} + \cos\phi \hat{\mathbf{p}}) E_x(y') e^{j(k \sin\theta \sin\phi - \beta)y'} dy' \right\}. \tag{45b}$$

These results are sufficient for radiation pattern calculations since the directivity from equation (41) is independent of amplitude scale factors.

We conduct a parametrical study to evaluate the influence of slot length and width on the far field radiation pattern at fixed frequency. For the waveguide and slot dimensions previously considered ($ka = 4.25, b = a/2$ and $d = b/30$), the H-plane (i.e., $\phi = \pi/2$) realized gain pattern is shown in figure 12 with aperture length as a parameter. The total efficiency is also shown corresponding to $\eta = -1.4, -0.8, -0.5$, and -0.3 dB. The pattern is as expected for an approximately uniform source distribution with SLL $\sim$ 13 dB. The beam appears at an angle that depends on the phase variation over the aperture, and this is completely determined from the variable aperture width. The azimuthal beam angle, $\phi_0 = \pi/2$, remains fixed and is referred to as the "forward" direction. For constant aperture width, the elevation beam angle, θ_0, is determined by the perturbed waveguide wavelength. As the aperture width approaches zero, the elevation beam angle approaches

$$\theta_0 = \sin^{-1}\left(\lambda_0/\lambda_{g0}\right) \sim 42^\circ \tag{46}$$

in which λ_{g0} is the guide wavelength for the unperturbed (i.e., closed) waveguide. This is shown in figure 13 for fixed slot length, $L = 20\lambda_0$, and

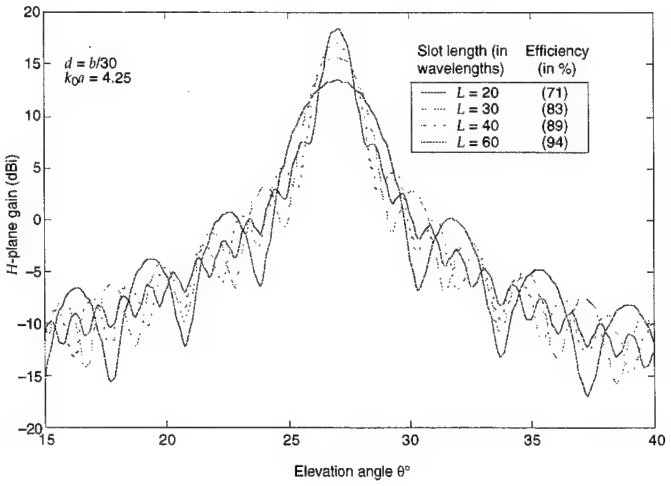

Figure 12. Realized gain for a constant width aperture in a waveguide narrow wall with length as a parameter.

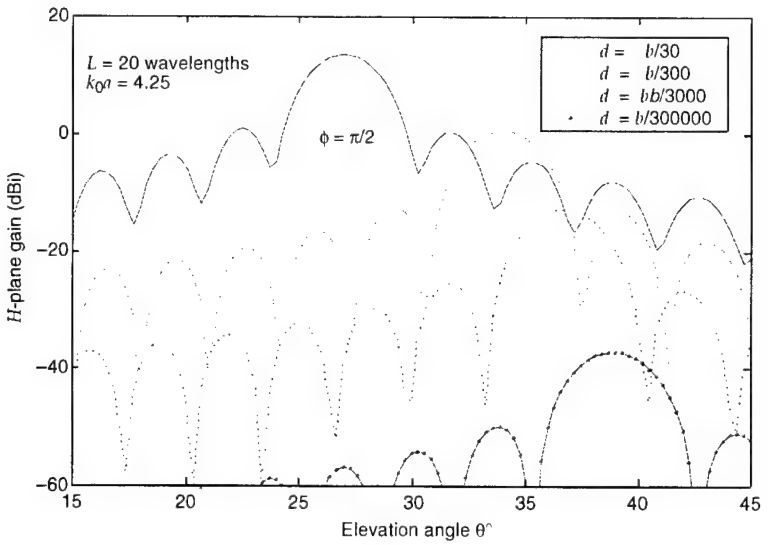

Figure 13. Realized gain for a constant width aperture in a waveguide narrow wall with width as a parameter.

decreasing slot width where the realized gain is reduced according to the total efficiency.

Now consider a specific example of a constant width aperture in the narrow wall of WR-284 waveguide where the interior dimensions are $a = 2.84$ in. and $b = 1.34$ in. (which is not half-height waveguide). The aperture width is constant at $d = b/25$ with length $L = 30a \sim 20\lambda_0$ at a frequency where $ka = 4.25$. The calculated gain at this frequency is shown as a function of the elevation angle and versus the azimuthal angle at fixed elevation. The H-plane gain with $\phi_0 = \pi/2$ is shown in figure 14a where the main beam angle, $\theta_0 = 24.7°$.

The realized gain versus azimuth at this fixed elevation angle is shown in figure 14b. The beam can be frequency scanned from broadside and remains free of grating lobes. The main beam angle from broadside (or overhead) when $\phi_0 = \pi/2$ is shown in figure 15 as a function of normalized frequency. The realized gain for WR-284 slotted waveguide (with $d = b/30$) is shown in figure 16 at three frequencies corresponding to $ka = 4.0$, 4.25, and 4.5, in which $\eta = -0.9, -1.3$, and -1.7 dB, respectively. The result indicates that the pattern is stable over this frequency BW with less than a 2-dB gain variation. The main beam can be positioned at a desired elevation angle by adjusting the guide phase constant and then frequency scanning over about 20° (for 12 percent BW). The corresponding peak gain, $G_r(\theta_0, \pi/2)$ and total efficiency are shown in figure 17a and 17b, respectively. To obtain the radiation pattern for a realistic aperture, the rectangular source distribution in two dimensions is required as in equation (37). However, for the narrow slots considered (without transverse currents), equation (45) is used since the radiation by a rectangular aperture source is a negligible correction of these line source results.

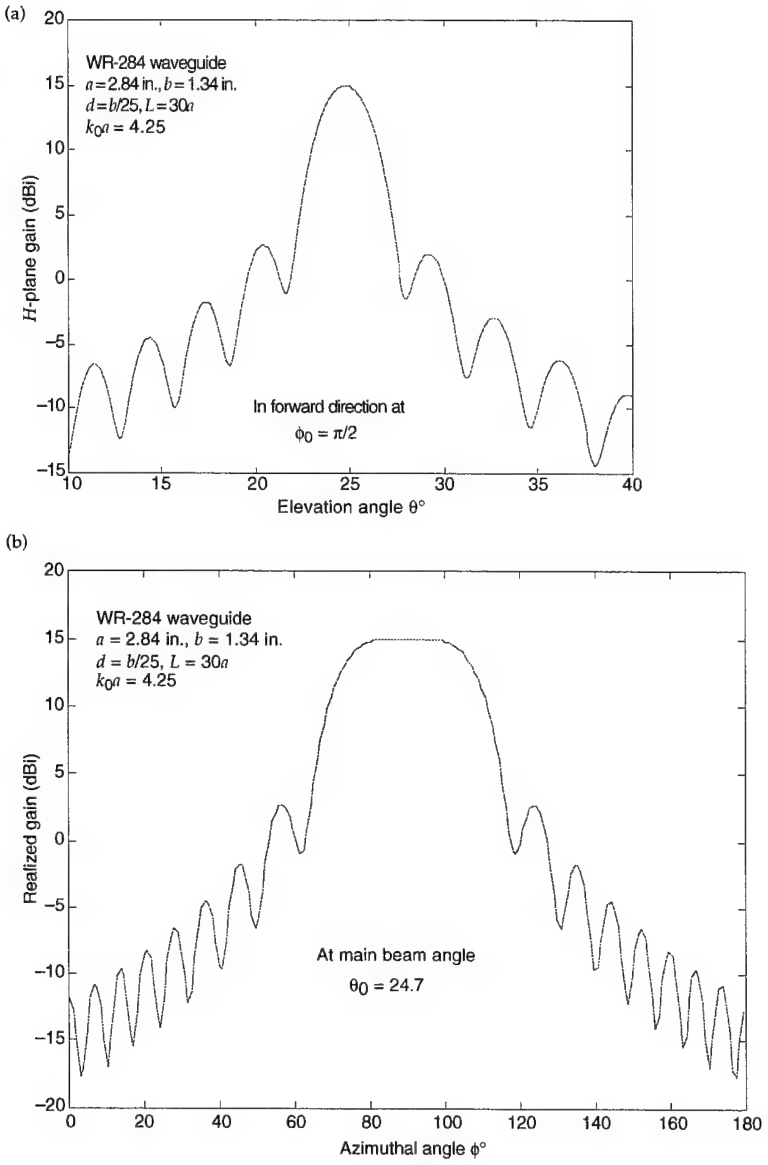

Figure 14. (a) H-plane realized gain for a constant width aperture in the narrow wall of WR-284 and (b) realized gain at the main beam angle for a constant width aperture in narrow wall of WR-284.

Figure 15. Main beam angle scan range for a constant width aperture in narrow wall of WR-284.

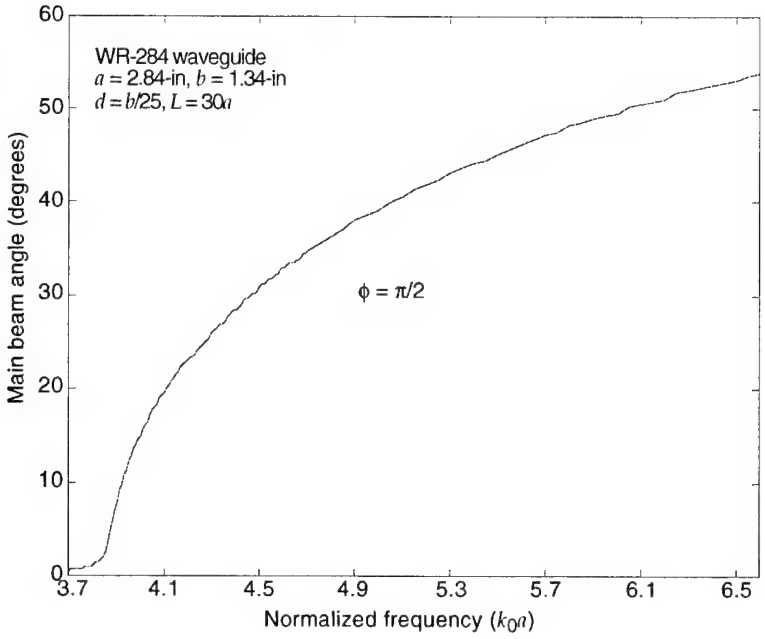

Figure 16. Calculated H-plane gain for an aperture in narrow wall of WR-284 waveguide.

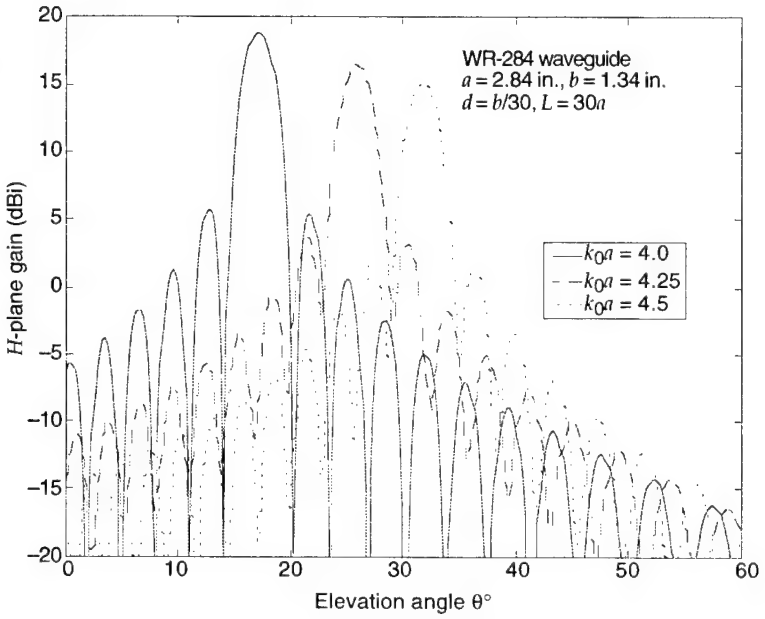

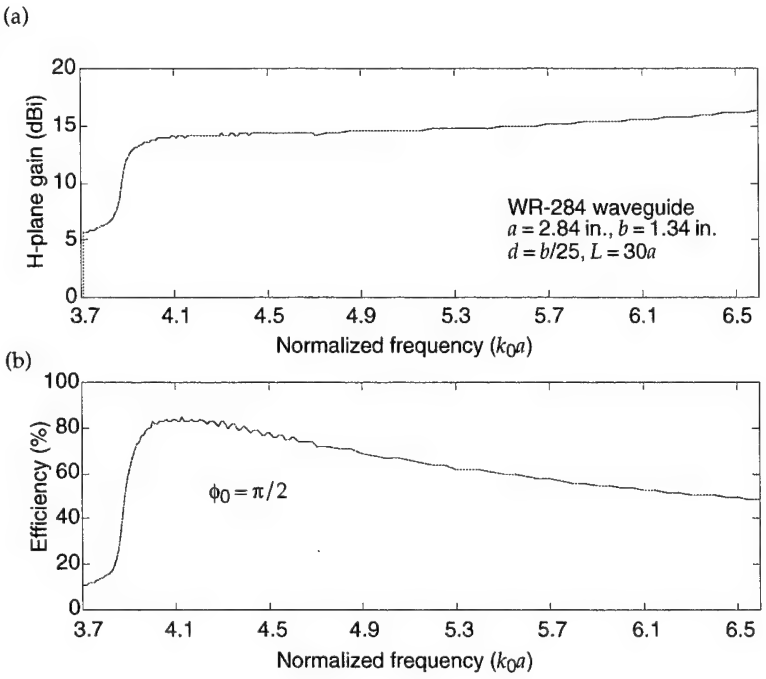

Figure 17. Results for a constant width aperture in narrow wall of WR-284 waveguide: (a) peak realized gain and (b) total efficiency.

5. Conclusion

Following Goldstone and Oliner [5], we have presented an equivalent circuit model for a narrow slot in a rectangular waveguide. The transverse resonance technique is applied to the resulting transmission line description to provide the resonance condition. The transcendental equation is then approximated by a perturbation solution resulting in the perturbed waveguide propagation constant. The waveguide attenuation constant determines the aperture distribution function that has the waveguide longitudinal phase variation. The radiated EM fields are then obtained by numerical integration over the aperture source, where the main beam angle depends on the perturbed waveguide phase constant. It was shown that a tapered (or flared) slot width corrupted the radiation pattern, so we consider only constant width slots in detail. Parametric results were shown for a constant width slot in WR-284 waveguide, which corresponds to a tapered aperture illumination function. The TE-slotted waveguide TWA has good radiation characteristics (i.e., $\eta > 70$ percent) over a frequency range corresponding to $ka = 4.0 - 4.5$ or rather, $ka = 4.25 \pm 6$ percent. Over this 12-percent frequency band (i.e., 2.65 to 2.98 GHz), the main beam scans 10° to 30° from broadside (or overhead). This scan range could be augmented with electronic control of the waveguide phase constant in order to phase scan the beam from broadside. In the sequel to (i.e., Part II) this report, dielectric loaded waveguides are considered in which voltage-controlled dielectric materials integrated into the antenna structure may allow efficient phase scanning of the slotted waveguide TWA.

References

1. Walter, C. H., *Traveling Wave Antennas*, McGraw-Hill Book Co., New York, 1965.

2. Marcurvitz, N. ed., *Waveguide Handbook*, McGraw-Hill Book Co., New York, 1951.

3. Wasylkiwskyj, W., "A Leaky-wave Dual Beam Antenna," *Inst. for Defense Analysis*, Washington, DC, (1979).

4. Stegan, R. J., and R. H. Reed, "Arrays of Closely Spaced Nonresonant Slots," *IRE Trans. Antennas Propagat.*, Vol. AP-2, pp 109–113, July 1954.

5. Goldstone, L. O., and A. A. Oliner, "Leaky-Wave Antennas I: Rectangular Waveguides," *IRE Trans. Antennas Propagat.*, Vol. AP-5, pp 307–319, October 1959.

6. Balanis, C. A., it Advanced Engineering Electromagnetics, John Wiley and Sons, Inc., New York, 1989.

7. Pozar, D. M., *Microwave Engineering*, 2nd ed., John Wiley and Sons, Inc., New York, 1998.

8. Jin, J., *The Finite Element Method in Electromagnetics*, John Wiley and Sons, Inc., New York, 1993.

Appendix A. Modal Decomposition in a Parallel Plate Region

Consider a parallel plate region of infinite extent with the coordinate system shown in figure A-1, where we presently locate the origin on the bottom plate. We desire a modal decomposition for electromagnetic (EM) fields having an exponential phase variation, $\mathbf{e}^{-j\beta_n y}$ in the propagation direction for the nth-mode. A modal decomposition in terms of transverse to y electric (TE-) and magnetic (TM-) fields is possible, but ultimately, we desire to include an aperture in the waveguide which perturbs the modal fields. In a typical TE-TM mode decomposition, separate transmission lines in the direction transverse to y are required to represent each mode, which are coupled by the presence of the aperture. We indicate this schematically in figure A-2, where an aperture fed by a parallel plate waveguide creates fringing fields that have E_x- and E_z-components. The mode would also have an E_y-component requiring a linear combination of TE- (or H-modes) and TM-modes to represent the EM field. Single mode decomposition is more attractive in order to obtain a single transverse transmission line representation for an aperture in rectangular waveguide. To this end, we use an alternate modal decomposition that will be helpful in the analysis of leaky wave guiding structures such as that shown in figure A-3.

We desire to construct a transmission line description of waves propagating in a direction transverse to the propagation direction, y in the parallel plate guide (i.e., the z-direction operator $\nabla_{tz} \equiv \frac{\partial}{\partial x}\hat{\mathbf{x}} + \frac{\partial}{\partial y}\hat{\mathbf{y}}$. From the Maxwell field equations, the EM fields must satisfy

$$-\frac{\partial \mathbf{E}_{tz}}{\partial z} = j\omega\mu \left[\bar{\bar{\mathbf{I}}} + \frac{\nabla_{tz}\nabla_{tz}}{k^2}\right] \cdot (\mathbf{H}_{tz} \times \hat{\mathbf{z}}) \tag{A-1a}$$

$$-\frac{\partial \mathbf{H}_{tz}}{\partial z} = j\omega\varepsilon \left[\bar{\bar{\mathbf{I}}} + \frac{\nabla_{tz}\nabla_{tz}}{k^2}\right] \cdot (\hat{\mathbf{z}} \times \mathbf{E}_{tz}) \tag{A-1b}$$

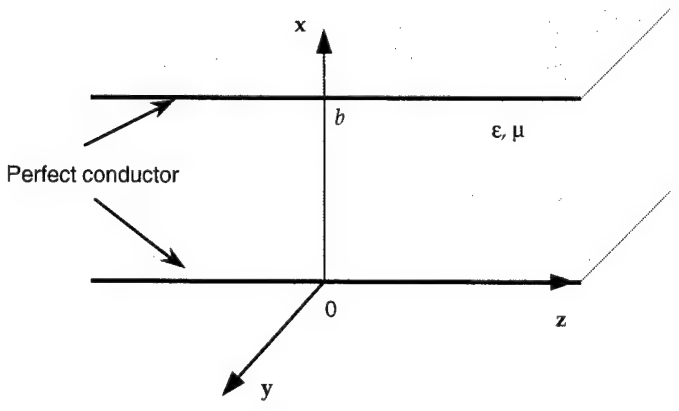

Figure A-1. An infinite parallel plate region.

Figure A-2. Parallel plate fed aperture.

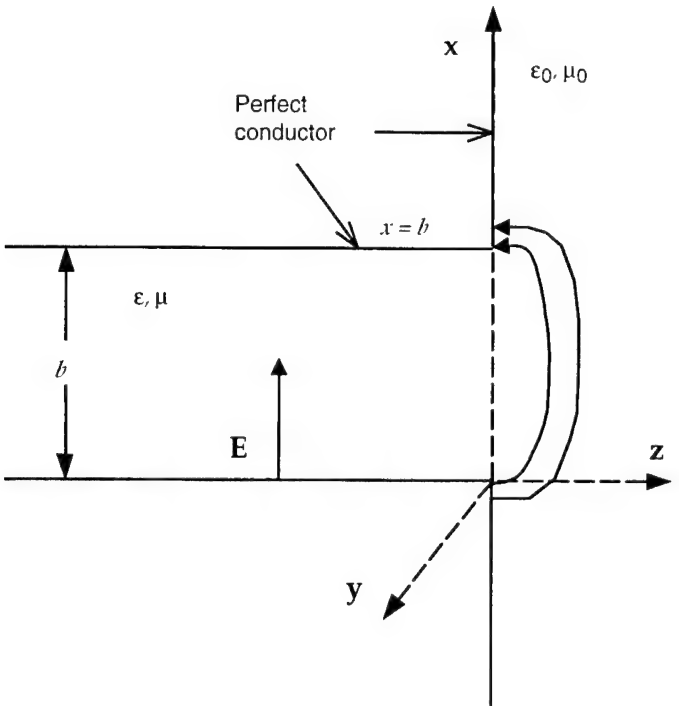

Figure A-3. An aperture in narrow wall of rectangular waveguide.

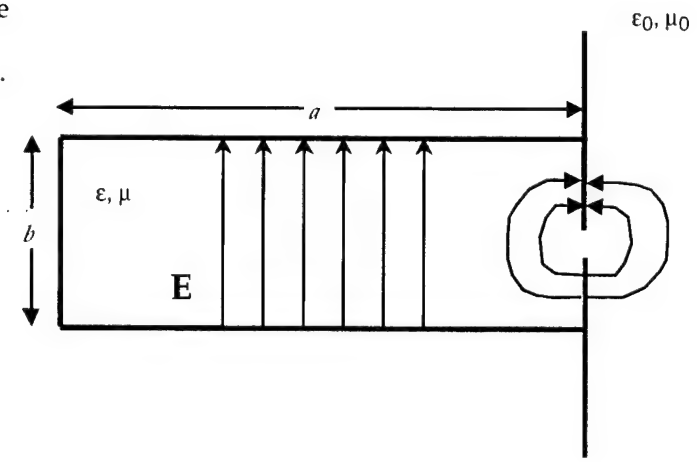

in which $\bar{\bar{\mathbf{I}}} = \hat{\mathbf{x}}\hat{\mathbf{x}} + \hat{\mathbf{y}}\hat{\mathbf{y}} + \hat{\mathbf{z}}\hat{\mathbf{z}}$ is the unit dyadic and

$$j\omega\mu H_z = \nabla_{tz} \cdot (\hat{\mathbf{z}} \times \mathbf{E}_{tz}) \tag{A-2a}$$

$$j\omega\varepsilon E_z = \nabla_{tz} \cdot (\mathbf{H}_{tz} \times \hat{\mathbf{z}}) \ . \tag{A-2b}$$

In the parallel plate region, $0 \leq x \leq b$, the medium has permeability, $\mu = \mu_0\mu_r$ and permittivity, $\epsilon = \epsilon_0\epsilon_r$, which are presently taken to be constants.

In the spirit of separation of variables, expand the transverse (to z) fields in vector modal functions that are constructed to have the correct x and y spatial variation,

$$\mathbf{E}_{tz}(x,y,z) = V_n(z)\mathbf{e}_n(x,y) \tag{A-3a}$$

$$\mathbf{H}_{tz}(x,y,z) = I_n(z)\mathbf{h}_n(x,y)\,. \tag{A-3b}$$

The $V_n(z)$ and $I_n(z)$ are the nth-mode amplitude functions that satisfy transmission line equations in the longitudinal direction,

$$-\frac{dV_n(z)}{dz} = jk_{zn}Z_nI_n(z) \tag{A-4a}$$

$$-\frac{dI_n(z)}{dz} = jk_{zn}Y_nV_n(z) \tag{A-4b}$$

in which $Z_n = 1/Y_n$ is the characteristic (wave) impedance and jk_{zn} the propagation constant along z corresponding to the nth-mode. When we use equation (A-3) in equation (A-1) and take account of equation (A-4), the transverse (to z) mode functions are

$$\mathbf{e}_n = \frac{\omega\mu}{k_{zn}Z_n}\left[\bar{\bar{\mathbf{I}}} + \frac{\nabla_{tz}\nabla_{tz}}{k^2}\right]\cdot(\mathbf{h}_n\times\hat{\mathbf{z}}) \tag{A-5a}$$

$$\mathbf{h}_n = \frac{\omega\varepsilon}{k_{zn}Y_n}\left[\bar{\bar{\mathbf{I}}} + \frac{\nabla_{tz}\nabla_{tz}}{k^2}\right]\cdot(\hat{\mathbf{z}}\times\mathbf{e}_n)\,. \tag{A-5b}$$

The transverse EM fields are then obtained from equation (A-3) in terms of the transmission line voltage and current functions. With equation (A-3) in equation (A-2), the "longitudinal" fields are

$$j\omega\mu H_z = V_n(z)\nabla_{tz}\cdot(\hat{\mathbf{z}}\times\mathbf{e}_n) \tag{A-6a}$$

$$j\omega\varepsilon E_z = I_n(z)\nabla_{tz}\cdot(\mathbf{h}_n\times\hat{\mathbf{z}})\,. \tag{A-6b}$$

With $\mathbf{e}_n = \mathbf{h}_n\times\hat{\mathbf{z}}$, the classical TE-TM modal decomposition could be obtained. Instead, we define the $\mathbf{e}_n$-mode function by

$$\mathbf{e}_n = e^{-j\beta_n y}\cos\left(\frac{n\pi x}{b}\right)\hat{\mathbf{x}} \equiv \psi_n\hat{\mathbf{x}}\,. \tag{A-7}$$

Substituting equation (A-7) into the right side of equation (A-5b), we obtain

$$\begin{aligned}\mathbf{h}_n &= \frac{\omega\varepsilon}{k_{zn}Y_n}\left[\bar{\bar{\mathbf{I}}} + \frac{\nabla_{tz}\nabla_{tz}}{k^2}\right]\cdot\hat{\mathbf{y}}\psi_n \\ &= \frac{\omega\varepsilon}{k_{zn}Y_n}\left[\hat{\mathbf{y}}\psi_n + \frac{\nabla_{tz}}{k^2}\frac{\partial\psi_n}{\partial y}\right] = \frac{\omega\varepsilon}{k_{zn}Y_n}\left[\hat{\mathbf{y}} - \frac{j\beta_n\nabla_{tz}}{k^2}\right]\psi_n\,.\end{aligned} \tag{A-8}$$

With $k^2 = \omega^2\mu\epsilon$ and $\Psi_n = \mathrm{e}^{-j\beta_n y}\cos\left(\frac{n\pi x}{b}\right)$, this becomes

$$\mathbf{h}_n = \frac{1}{k_{zn}Y_n}\left[\frac{j\beta_n}{\omega\mu}\left(\frac{n\pi}{b}\right)\sin\left(\frac{n\pi x}{b}\right)\hat{\mathbf{x}} + \frac{k^2-\beta_n^2}{\omega\mu}\cos\left(\frac{n\pi x}{b}\right)\hat{\mathbf{y}}\right]e^{-j\beta_n y}\,. \tag{A-9}$$

The normal component vanishes at $x = 0$ and $x = b$, as required by a perfectly conducting boundary. To show that equations (A-9) and (A-7) are mutually consistent, substitute equation (A-9) into the right side of equation (A-5a) to obtain

$$\omega\mu\left[\bar{\bar{\mathbf{I}}}+\frac{\nabla_{tz}\nabla_{tz}}{k^2}\right]\cdot(\mathbf{h}_n\times\hat{\mathbf{z}})=\omega\mu\left[\bar{\bar{\mathbf{I}}}+\frac{\nabla_{tz}\nabla_{tz}}{k^2}\right] \tag{A-10}$$
$$\cdot\left[\frac{k^2-\beta_n^2}{\omega\mu}\cos\left(\frac{n\pi x}{b}\right)\hat{\mathbf{x}}-\frac{j\beta_n}{\omega\mu}\left(\frac{n\pi}{b}\right)\sin\left(\frac{n\pi x}{b}\right)\hat{\mathbf{y}}\right]\frac{e^{-j\beta_n y}}{k_{zn}Y_n}\,.$$

When we take derivatives and cancel terms, equation (A-10) becomes

$$\frac{\omega\mu}{k_{zn}Y_n}\left\{\begin{array}{l}\left[\frac{k^2-\beta_n^2}{\omega\mu}\cos\left(\frac{n\pi x}{b}\right)\hat{\mathbf{x}}-\frac{j\beta_n}{\omega\mu}\left(\frac{n\pi}{b}\right)\sin\left(\frac{n\pi x}{b}\right)\hat{\mathbf{y}}\right]e^{-j\beta_n y}\\ +\frac{\nabla_{tz}}{\omega\mu k^2}\left[-k^2\left(\frac{n\pi}{b}\right)\sin\left(\frac{n\pi x}{b}\right)e^{-j\beta_n y}\right]\end{array}\right\}$$
$$=\frac{1}{k_{zn}Y_n}\left[k^2-\beta_n^2-\left(\frac{n\pi}{b}\right)^2\right]\cos\left(\frac{n\pi x}{b}\right)\hat{\mathbf{x}}e^{-j\beta_n y}\,. \tag{A-11}$$

Then the result in equation (A-11) must equal the left side of equation (A-5a). This gives the condition

$$k_{zn}^2=k^2-\beta_n^2-\left(\frac{n\pi}{b}\right)^2 \tag{A-12}$$

on the wavenumber for the transverse (to y) transmission line. The normalization factor is the characteristic impedance, chosen so that the y-component of the $\mathbf{h}_n$ mode function is simply ψ_n. From equation (A-9), this requires that

$$\frac{k^2-\beta_n^2}{k_{zn}Y_n\omega\mu}=1\quad\text{or } Z_n=\frac{k_{zn}\omega\mu}{k^2-\beta_n^2}\,. \tag{A-13}$$

With this normalization, the electric mode functions are from equation (A-7)

$$\mathbf{e}_n=\cos\left(\frac{n\pi x}{b}\right)\hat{\mathbf{x}}e^{-j\beta_n y} \tag{A-14a}$$

and from equation (A-9), the magnetic vector mode functions are

$$\mathbf{h}_n=\left[\frac{j\beta_n}{k^2-\beta_n^2}\left(\frac{n\pi}{b}\right)\sin\left(\frac{n\pi x}{b}\right)\hat{\mathbf{x}}+\cos\left(\frac{n\pi x}{b}\right)\hat{\mathbf{y}}\right]e^{-j\beta_n y}\,. \tag{A-14b}$$

The transverse fields are found from equation (A-3) and are simply the transverse mode functions with transmission line amplitudes. The corresponding longitudinal components are obtained when equation (A-14) is used in equation (A-6) and when we take account of equation (A-4). The result is

$$H_{zn}=-\left(\frac{\beta_n}{\omega\mu}\right)V_n(z)\cos\left(\frac{n\pi x}{b}\right)e^{-j\beta_n y} \tag{A-15a}$$

$$E_{zn}=\left(\frac{j\omega\mu}{k^2-\beta_n^2}\right)\left(\frac{n\pi}{b}\right)I_n(z)\sin\left(\frac{n\pi x}{b}\right)e^{-j\beta_n y}\,. \tag{A-15b}$$

This mode is a linear combination of a TE-mode and a TM-mode, often referred to as an H-type hybrid mode. The H-type mode characteristic

impedance is denoted Z_Hn, to have a clear distinction from the TE (or H-mode) case. We find the fundamental mode impedance from equation (A-13) using equation (A-12) with $n = 0$,

$$Z_{H0} = \frac{k_{z0}^2 \omega\mu}{k^2 - \beta_0^2} = \frac{\omega\mu}{k_{z0}} \,. \tag{A-16}$$

When $n = 0$ in equations (A-14) and (A-15), the H-type mode functions degenerate into

$$\mathbf{e}_0 = \hat{\mathbf{x}} e^{-j\beta_0 y} \,, \quad \text{and} \tag{A-17a}$$

$$\mathbf{h}_0 = \hat{\mathbf{y}} e^{-j\beta_0 y} \,, \quad \text{with} \tag{A-17b}$$

$$H_{0n} = -\left(\frac{\beta_0}{\omega\mu}\right) V_0(z) e^{-j\beta_0 y} \tag{A-17c}$$

Thus, the fundamental H-type mode is equivalent to an H_{10}-mode propagating in the y-direction. The H-type mode decomposition is useful in the analysis of leaky wave antennas such as an aperture in the narrow wall of rectangular waveguide (see fig. A-3). The H-type mode decomposition in the transverse direction has a fundamental mode that can represent an incident H_{10}-mode. The aperture perturbation on this incident mode can then be described as introducing higher order H-type modes.

Appendix B. Equivalent Circuit Parameters for a Leaky H_{10} Rectangular Waveguide

We desire equivalent circuit parameters for a parallel plate waveguide fed aperture radiating into a half-space as shown in figure B-1. To follow convention, the origin is presently located on the bottom plate. The case of interest is an aperture in the narrow wall of a rectangular waveguide when excited by the H_{10}- (or TE_{10}-) mode. The unperturbed waveguide propagates the H_{10}-mode, but when the waveguide is perturbed by an aperture, an H-type hybrid mode is appropriate as developed in appendix A. The H-type modal decomposition in the transverse direction reduces to the H_{10} case when $n = 0$ as shown in equation (A-17). Then, TE-excitation can be viewed as a fundamental H-type mode incident on the aperture plane, and the aperture perturbation produces higher order modes. Energy propagation along y in the parallel plate region can be viewed as a TEM wave incident at some angle, θ to the aperture (xy) plane as shown in figure B-2.

As in appendix A, take the z-axis as a propagation direction and consider transverse field components incident on the xy-plane. The electric (E-) field is polarized along the x-axis and is incident at an oblique angle to the aperture plane (see fig. B-2)

$$\mathbf{E}^{\text{inc}} = \hat{\mathbf{x}} e^{-jk_{y0}y - jk_{z0}z} \tag{B-1}$$

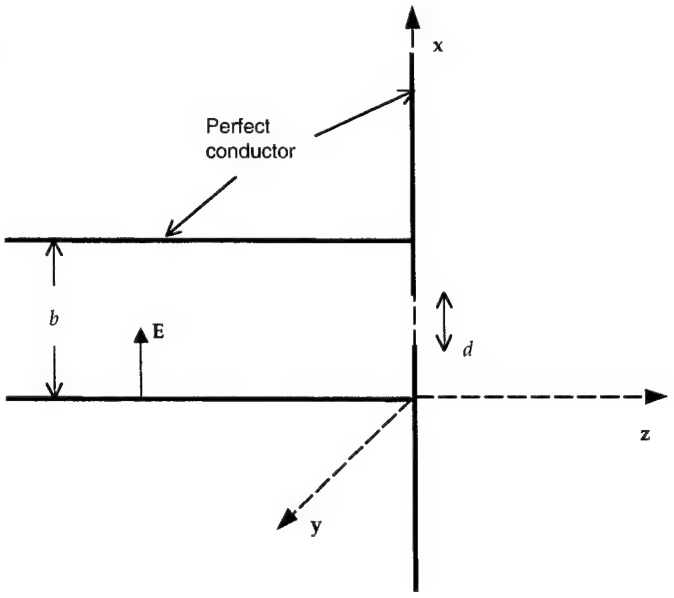

Figure B-1. TE-excited aperture radiating into a half-space (side view).

Figure B-2. TEM-wave incident at an oblique angle.

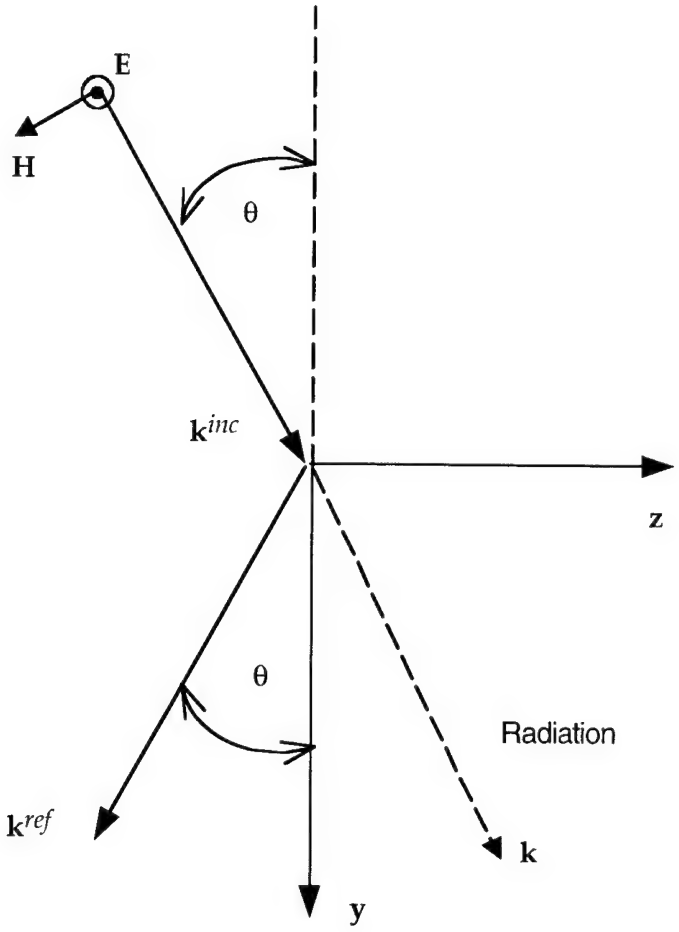

From Faraday's Law, the incident magnetic (H-) field is

$$\mathbf{H}^{\text{inc}} = \hat{\mathbf{y}}\frac{k_{z0}}{\omega\mu_0}e^{-jk_{y0}y-jk_{z0}z} - \hat{\mathbf{z}}\frac{k_{y0}}{\omega\mu_0}e^{-jk_{y0}y-jk_{z0}z} \tag{B-2}$$

in which only the transverse (to z) component is required in this analysis. For an air-filled waveguide, the components of the propagation constant are $jk_{y0} \equiv j\beta_0 = jk\cos\theta$ and $jk_{z0} = jk\sin\theta$. The wavenumber magnitude is then

$$k = \sqrt{\beta_0^2 + k_{z0}^2} \tag{B-3}$$

with longitudinal wavenumber, k_{z0}, of the transverse (to y) transmission line.

These incident electromagnetic (EM) fields correspond to the fundamental ($n = 0$) mode of an H-type modal decomposition as developed in appendix A. Using $\mathbf{E}^{\text{inc}}$ from equation (B-1) in equations (A-1b) and (A-2b), the incident magnetic (H-) field is that of the fundamental H-type mode equivalent to equations (A-17b) and (A-17c), but propagating at some oblique angle to the z-axis. This is because the mode amplitudes satisfy the transmission line equation (A-4) so the fields that are transverse to the propagation direction are related by the H-type mode characteristic (wave) impedance equation (A-13). Then the transverse component in equation (B-2) can be written in

terms of the fundamental mode wave impedance, $Z_{H0} = \omega\mu_0/k_{z0}$. Higher order H-type modes for the variation along x also satisfy the boundary conditions on the perfectly conducting surfaces when $k_{xn} = (n\pi/b)$. Since there is no variation of the waveguide along y, the wavenumber in this direction is the same for all n or $\beta_n = \beta_0 \equiv \beta$. For the nth-mode, the wavenumber magnitude of the transmission line along the z-axis is thus

$$k_{zn} = \sqrt{k^2 - \left(\frac{n\pi}{b}\right)^2 - \beta^2}\,. \tag{B-4}$$

The transverse modal decomposition in appendix A showed in equation (A-17) that the fundamental H-type mode degenerates to an H_{10}-mode propagating along y. Then the incident EM fields that are transverse to z can be described by an H_{10}-mode propagating along $\mathbf{k}^{\text{inc}}$ (see fig. B-2). The incident EM fields transverse to z can be written

$$\mathbf{E}^{\text{inc}} = \hat{\mathbf{x}} e^{-j\beta y - jk_{z0}z}\,, \quad \text{and} \tag{B-5a}$$

$$\mathbf{H}^{\text{inc}} = \hat{\mathbf{y}} \frac{e^{-j\beta y - jk_{z0}z}}{Z_{H0}} \tag{B-5b}$$

corresponding to a TEM wave incident at an oblique angle. These incident fields are partially reflected along the aperture with higher order modes generated according to the aperture reflection coefficient, Γ_n, for each $H-$type mode. The total EM fields within the waveguide are then a superposition of the incident field and an infinite sum of reflected modes. The total internal (i.e., $z \leq 0$) E-field transverse to z is

$$\mathbf{E}_{tz}^{\text{int}} = \hat{\mathbf{x}} \left[\left(e^{-jk_{z0}z} + \Gamma_0 e^{jk_{z0}z} \right) + \sum_{n=1}^{\infty} \Gamma_n \cos\left(\frac{n\pi x}{b}\right) e^{jk_{zn}z} \right] e^{-j\beta y}\,. \tag{B-6a}$$

The total transverse H-field is found with equation (A-5b) for the transverse mode functions by the inclusion of the sum of reflected modes. The result is as in equation (A-14b) for the $\mathbf{h}_n$-mode function or

$$\mathbf{H}_{tz}^{\text{int}} = \left\{ \begin{array}{l} \hat{\mathbf{y}} \frac{\left(e^{-jk_{z0}z} - \Gamma_0 e^{jk_{z0}z}\right)}{Z_{H0}} \\ -\sum_{n=1}^{\infty} \frac{\Gamma_n e^{jk_{zn}z}}{Z_{Hn}} \left[\frac{j\beta}{k_0^2 - \beta^2} \left(\frac{n\pi}{b}\right) \sin\left(\frac{n\pi x}{b}\right) \hat{\mathbf{x}} + \cos\left(\frac{n\pi x}{b}\right) \hat{\mathbf{y}} \right] \end{array} \right\} e^{-j\beta y}\,. \tag{B-6b}$$

where the wave impedance is that for the H-type waveguide mode

$$Z_{Hn} = \frac{k_{zn}\omega\mu_0}{k^2 - \beta^2} = \frac{k_{zn}\omega\mu_0}{k_{zn}^2 + \left(\frac{n\pi}{b}\right)^2}\,. \tag{B-7}$$

The longitudinal (z-) field components can be found with equation (A-6) but are not required here.

For $z \geq 0$, the total EM fields can be written as a superposition of complex exponential functions corresponding to a Fourier integral with the transform variable being the transverse wavenumber. With longitudinal and transverse components of the k-vector, $\mathbf{k} = \mathbf{k}_z + \mathbf{k}_t$, the radiated fields are

$$\mathbf{E}^{\text{ext}} = \int_{-\infty}^{\infty}\int_{-\infty}^{\infty} \tilde{\mathbf{E}}\left(\mathbf{k}_t\right) e^{-jk_x x - jk_y y - j\sqrt{k_0^2 - k_x^2 - k_y^2}z} \frac{dk_x dk_y}{(2\pi)^2} \ , \quad \text{and} \tag{B-8a}$$

$$\mathbf{H}^{\text{ext}} = \int_{-\infty}^{\infty}\int_{-\infty}^{\infty} \frac{\mathbf{k} \times \tilde{\mathbf{E}}\left(\mathbf{k}_t\right)}{\omega\mu_0} e^{-jk_x x - jk_y y - j\sqrt{k_0^2 - k_x^2 - k_y^2}z} \frac{dk_x dk_y}{(2\pi)^2} \ . \tag{B-8b}$$

The wavenumber along the aperture is that of the waveguide mode, $k_y = \beta$ for all n or

$$\tilde{\mathbf{E}}(\mathbf{k}_t) = 2\pi\tilde{\mathbf{E}}(k_x)\delta\left(k_y - \beta\right) \ . \tag{B-9}$$

Then the external EM fields are found from equation (B-8) via the amplitude coefficients in equation (B-9)

$$\mathbf{E}^{\text{ext}} = \frac{e^{-j\beta y}}{2\pi} \int_{-\infty}^{\infty} \tilde{\mathbf{E}}\left(k_x\right) \mathrm{e}^{-jk_x x - jk_z z} dk_x \ , \quad \text{and} \tag{B-10a}$$

$$\mathbf{H}^{\text{ext}} = \frac{e^{-j\beta y}}{2\pi\omega\mu_0} \int_{-\infty}^{\infty} \left(k_x\hat{\mathbf{x}} + \beta\hat{\mathbf{y}} + k_z\hat{\mathbf{z}}\right) \times \tilde{\mathbf{E}}\left(k_x\right) e^{-jk_x x - jk_z z} dk_x \tag{B-10b}$$

where the longitudinal wavenumber magnitude is

$$k_z = \sqrt{k^2 - k_x^2 - \beta^2} \quad \text{or} \ k_x^2 + k_z^2 = k^2 - \beta^2 \ . \tag{B-11}$$

Since the component of the wavenumber along the aperture length, β, is fixed, the amplitude coefficient can be written

$$\tilde{\mathbf{E}}(k_x) = \mathcal{E}_x(k_x)\hat{\mathbf{x}} + \mathcal{E}_z(k_x)\hat{\mathbf{z}} \ . \tag{B-12}$$

Further, there is no component of E-field along the k-vector in the radiation direction, $\mathbf{k}$, so we can eliminate one component of the amplitude coefficient by recognizing that $\mathbf{k} \bullet \tilde{\mathbf{E}} = 0$ or

$$k_x\mathcal{E}_x + k_z\mathcal{E}_z = 0 \quad \text{so} \ \mathcal{E}_z = -\left(\frac{k_x}{k_z}\right)\mathcal{E}_x \ . \tag{B-13}$$

The cross product in equation (B-8b) is then

$$\begin{aligned} \mathbf{k} \times \tilde{\mathbf{E}} &= \left[\mathcal{E}_z\beta\hat{\mathbf{x}} + \left(k_z\mathcal{E}_x - k_x\mathcal{E}_z\right)\hat{\mathbf{y}} - \beta\mathcal{E}_x\hat{\mathbf{z}}\right] \\ &= \left[\left(-\frac{\beta k_x}{k_z}\right)\hat{\mathbf{x}} + \frac{k^2 - \beta^2}{k_z}\hat{\mathbf{y}} - \beta\hat{\mathbf{z}}\right]\mathcal{E}_x \ . \end{aligned} \tag{B-14}$$

The external EM fields can be written in terms of this single component of the Fourier transform variable, with the result

$$\mathbf{E}^{\text{ext}} = \frac{e^{-j\beta y}}{2\pi}\hat{\mathbf{x}} \int_{-\infty}^{\infty} \mathcal{E}_x e^{-jk_x x - jk_z z} dk_x - \frac{e^{-j\beta y}}{2\pi}\hat{\mathbf{z}} \int_{-\infty}^{\infty} \mathcal{E}_x \frac{k_x}{k_z} e^{-jk_x x - jk_z z} dk_x \ , \quad \text{and} \tag{B-15a}$$

$$\begin{aligned} \mathbf{H}^{\text{ext}} &= -\frac{\beta e^{-j\beta y}}{2\pi\omega\mu_0}\hat{\mathbf{x}} \int_{-\infty}^{\infty} \frac{k_x}{k_z}\mathcal{E}_x e^{-jk_x x - jk_z z} dk_x \\ &+ \frac{k_0^2 - \beta^2}{2\pi\omega\mu_0} e^{-j\beta y}\hat{\mathbf{y}} \int_{-\infty}^{\infty} \frac{\mathcal{E}_x}{k_z} e^{-jk_x x - jk_z z} dk_x - \frac{\beta e^{-j\beta y}}{2\pi\omega\mu_0}\hat{\mathbf{z}} \int_{-\infty}^{\infty} \mathcal{E}_x e^{-jk_x x - jk_z z} dk_x \ . \end{aligned} \tag{B-15b}$$

Then the external fields that are transverse to z are

$$\mathbf{E}_{tz}^{\text{ext}} = \frac{e^{-j\beta y}}{2\pi}\hat{\mathbf{x}}\int_{-\infty}^{\infty}\mathcal{E}_x e^{-jk_x x - jk_z z}dk_x\,, \quad \text{and} \tag{B-16a}$$

$$\mathbf{H}_{tz}^{\text{ext}} = -\frac{\beta e^{-j\beta y}}{2\pi\omega\mu_0}\hat{\mathbf{x}}\int_{-\infty}^{\infty}\frac{k_x}{k_z}\mathcal{E}_x e^{-jk_x x - jk_z z}dk_x + \frac{k_0^2-\beta^2}{2\pi\omega\mu_0}e^{-j\beta y}\hat{\mathbf{y}}\int_{-\infty}^{\infty}\frac{\mathcal{E}_x}{k_z}e^{-jk_x x - jk_z z}dk_x\,. \tag{B-16b}$$

The boundary condition on the internal and external fields at the aperture plane requires continuity of the tangential (i.e., transverse to z) field components. Then equating equations (B-6) and (B-16) and omitting the common factor $e^{-j\beta y}$, we must have at $z = 0$

$$1 + \Gamma_0 + \sum_{n=1}^{\infty}\Gamma_n\cos\left(\frac{n\pi x}{b}\right) = \frac{1}{2\pi}\int_{-\infty}^{\infty}\mathcal{E}_x e^{-jk_x x}dk_x\,, \tag{B-17a}$$

$$\sum_{n=1}^{\infty}\frac{j\beta}{k_{z0}^2}\left(\frac{n\pi}{b}\right)\frac{\Gamma_n}{Z_{Hn}}\sin\left(\frac{n\pi x}{b}\right) = \frac{-\beta}{2\pi\omega\mu_0}\int_{-\infty}^{\infty}\frac{k_x}{k_z}\mathcal{E}_x e^{-jk_x x}dk_x\,, \quad \text{and} \tag{B-17b}$$

$$\frac{1-\Gamma_0}{Z_{H0}} - \sum_{n=1}^{\infty}\frac{\Gamma_n}{Z_{Hn}}\cos\left(\frac{n\pi x}{b}\right) = \frac{k_{z0}^2}{2\pi\omega\mu_0}\int_{-\infty}^{\infty}\frac{\mathcal{E}_x}{k_z}e^{-jk_x x}dk_x \tag{B-17c}$$

using the relation, $k_{z0}^2 = k^2 - \beta^2$. For the nth-mode we have

$$k_{zn} = \sqrt{k_{z0}^2 - \left(\frac{n\pi}{b}\right)^2} = -j\sqrt{\left(\frac{n\pi}{b}\right)^2 - k_{z0}^2} = -j\sqrt{\left(\frac{n\pi}{b}\right)^2 - k^2\sin^2\theta} \tag{B-18}$$

Then using equation (B-18) along with equation (B-7), we find that equation (B-17b) becomes

$$\sum_{n=1}^{\infty}\frac{\frac{n\pi}{b}\Gamma_n}{\sqrt{\left(\frac{n\pi}{b}\right) - k^2\sin^2\theta}}\sin\left(\frac{n\pi x}{b}\right) = \frac{1}{2\pi}\int_{-\infty}^{\infty}\frac{k_x}{k_z}\mathcal{E}_x e^{-jk_x x}dk_x\,. \tag{B-19}$$

The aperture E-field at $z = 0$, $E_{xA}(x,0)$, is the one-dimensional Fourier transform that appears on the right side of equation (B-17a). We have the Fourier transform pairs

$$E_{x\text{A}}(x) = \frac{1}{2\pi}\int_{-\infty}^{\infty}\mathcal{E}_x e^{-jk_x x}dk_x\,, \quad \text{and} \tag{B-20a}$$

$$\mathcal{E}_x = \frac{1}{2\pi}\int_{\text{Ap}}E_{x\text{A}}(x')e^{jk_x x'}dx' \tag{B20b}$$

in which the second integral extends only over the aperture. Using equation (B-7), we find that the condition equation (B-17c) becomes

$$1-\Gamma_0-\sum_{n=1}^{\infty}\frac{Z_{H0}}{Z_{Hn}}\Gamma_n\cos\left(\frac{n\pi x}{b}\right)=\frac{k_{z0}}{2\pi}\int_{-\infty}^{\infty}\frac{e^{-jk_x x}}{k_z}dk_x\int_{\mathrm{Ap}}E_{x\mathrm{A}}\left(x'\right)e^{-jk_x x'}dx'$$

$$=\frac{k_{z0}}{2\pi}\int_{\mathrm{Ap}}E_{x\mathrm{A}}\left(x'\right)dx'\int_{-\infty}^{\infty}\frac{e^{-jk_x(x-x')}}{\sqrt{k_{z0}^2-\beta^2}}dk_x=\frac{k_{z0}}{2}\int_{\mathrm{Ap}}H_0^{(2)}\left(k_{z0}\left|x-x'\right|\right)E_{x\mathrm{A}}\left(x'\right)dx' \qquad \text{(B-21)}$$

in which $H_\nu^{(2)}$ is the Hankel function of the second kind, order ν. An expression for Γ_n can be obtained from equation (B-17b), but this is not required when one is using orthogonal mode functions.

We can take advantage of orthogonal functions to further simplify the results. For now, assume that the aperture is the full waveguide opening or $d = b$ in figure B-2. Multiply both sides of equation (B-17a) by $\cos(n\pi x/b), n \geq 1$ and integrate over the aperture width, b. The result is an expression for Γ_n

$$\frac{b}{2}\Gamma_n=\int_0^b E_{xA}(x')\cos\left(\frac{n\pi x'}{b}\right)dx',\quad n\geq 1\,. \qquad \text{(B-22a)}$$

Taking the complex conjugate of equation (B-22a), we have also

$$\frac{b}{2}\Gamma_n^*=\int_0^b E_{xA}^*(x')\cos\left(\frac{n\pi x'}{b}\right)dx',\quad n\geq 1\,. \qquad \text{(B-22b)}$$

By directly integrating both sides of equation (B-17a) with respect to x, we obtain an expression for Γ_0

$$(1+\Gamma_0)b=\int_0^b E_{x\mathrm{A}}(x')dx'\,. \qquad \text{(B-23)}$$

Now multiply equation (B-21) by the conjugate of the aperture field, $E_{x\mathrm{A}}^*$, and integrate with respect to x using equation (B-22b) to find

$$(1-\Gamma_0)\int_0^b E_{x\mathrm{A}}^*(x)dx-\frac{b}{2}\sum_{n=1}^{\infty}\frac{|\Gamma_n|^2 Z_{H0}}{Z_{Hn}}=\frac{k_{z0}}{2}\int_0^b dx\int_0^b H_0^{(2)}\left(k_{z0}\left|x-x'\right|\right)E_{x\mathrm{A}}^*(x)E_{x\mathrm{A}}(x')dx'\,. \qquad \text{(B-24)}$$

Dividing by $\int_0^b E_{x\mathrm{A}}^*(x)dx$ and transposing terms, we have

$$(1-\Gamma_0)=\frac{\frac{b}{2}\sum_{n=1}^{\infty}\frac{|\Gamma_n|^2 Z_{H0}}{Z_{Hn}}+\frac{k_{z0}}{2}\int_0^b dx\int_0^b dx' H_0^{(2)}\left(k_{z0}\left|x-x'\right|\right)E_{x\mathrm{A}}^*(x)E_{x\mathrm{A}}\left(x'\right)}{\int_0^b E_{x\mathrm{A}}^*(x)dx}\,. \qquad \text{(B-25)}$$

Dividing equation (B-25) by equation (B-23) gives

$$\frac{1-\Gamma_0}{1+\Gamma_0}=\frac{\frac{b^2}{2}\sum_{n=1}^{\infty}\frac{Z_{H0}}{Z_{Hn}}|\Gamma_n|^2+\frac{k_{z0}b}{2}\int_0^b dx\int_0^b dx' H_0^{(2)}\left(k_{z0}\left|x-x'\right|\right)E_{x\mathrm{A}}^*(x)E_{x\mathrm{A}}(x')}{\left|\int_0^b E_{x\mathrm{A}}(x')dx'\right|^2}\,. \qquad \text{(B-26)}$$

The input admittance at $z = 0$ is defined in terms of the reflection coefficient [3, p 14], or

$$\frac{Y_{\text{in}}}{Y_{H0}} = \frac{1 - \Gamma_0}{1 + \Gamma_0} \tag{B-27}$$

in which $Y_{H0} = 1/Z_{H0}$ is the characteristic admittance. Using equations (B-4) and (B-7) with $n = 0$, we also note that $Z_{Hn} = k_{zn}\omega\mu_0/k_{z0}^2$ so that

$$\frac{Z_{H0}}{Z_{Hn}} = \frac{k_{z0}}{k_{zn}} . \tag{B-28}$$

Substitute equation (B-22a) for Γ_n in equation (B-26), and using equations (B-27) and (B-28) we get

$$\frac{Y_{\text{in}}}{Y_{H0}} = \frac{2\sum_{n=1}^{\infty} \frac{k_{z0}}{k_{zn}} \left| \int_0^b E_{x\text{A}}(x) \cos\left(\frac{n\pi x}{b}\right) dx \right|^2 + \frac{k_{z0}b}{2} \int_0^b dx \int_0^b dx' H_0^{(2)}\left(k_{z0}\left|x - x'\right|\right) E_{x\text{A}}^*(x) E_{x\text{A}}(x')}{\left| \int_0^b E_{x\text{A}}(x') dx' \right|^2} \tag{B-29}$$

which is a variational expression for the input admittance. If we assume a constant aperture field, $E_{x\text{A}}(x) = E_{x\text{A}}$, then the first term on the right side of equation (B-29) vanishes and so an approximate expression for the input admittance in this case (i.e., H_{10}-excitation) is

$$\frac{Y_{\text{in}}}{Y_{H0}} \cong \frac{k_{z0}}{2b} \int_0^b dx \int_0^b dx' H_0^{(2)}\left(k_{z0}\left|x - x'\right|\right) . \tag{B-30}$$

In terms of the dimensionless variable $\chi = k_{z0}x = kx\sin\theta$, we have

$$\frac{Y_{\text{in}}}{Y_{H0}} \cong \frac{1}{2k_{z0}b} \int_0^{k_{z0}b} d\chi \int_0^{k_{z0}b} d\chi' H_0^{(2)}\left(\left|\chi - \chi'\right|\right) . \tag{B-31}$$

This result is a Green's function type integral in which the integrand depends only on the absolute value of the difference parameter, $\eta = |\chi - \chi'|$, so is an even function of η. In general, we are interested in an integral of the form, $\mathbf{I} \equiv \int_0^b \int_0^b \mathrm{f}(\chi - \chi') d\chi d\chi'$ in a square parameter space $0 < \chi < b$ and $0 < \chi' < b$. Define the difference parameter as $\eta = \chi - \chi'$ and let $\xi = \chi'$; then as shown in figure B-3, the parameter space transforms to $0 < \xi < b$ and $-\xi < \eta < b - \xi$. We integrate a strip over η in region 1 and region 2 where η assumes positive or negative values, respectively. Referring to figure B-3, the double integral becomes

$$\mathbf{I} = \int_0^b \mathrm{f}(\eta)\, d\eta \int_0^{b-\eta} d\xi + \int_{-b}^0 \mathrm{f}(\eta) d\eta \int_{-\eta}^b d\xi = \int_0^b \left\{\mathrm{f}(\eta) + f(-\eta)\right\}(b - \eta)\, d\eta . \tag{B-32}$$

Thus if $\mathrm{f}(\eta)$ is an even function of η, then equation (B-32) reduces to

$$\mathbf{I} = 2b \int_0^b \mathrm{f}(\eta) d\eta - 2 \int_0^b \eta \mathrm{f}(\eta) d\eta . \tag{B-33}$$

Now with $b = k_{z0}b$, let $\eta = k_{z0}(x - x')$ so that $\mathrm{f}(\eta) = H_0^{(2)}\left(k_{z0}\left|x - x\prime\right|\right)$, is an even function of η. Then with equation (B-33) with $\xi_0 = 120\pi\ \Omega$ the free

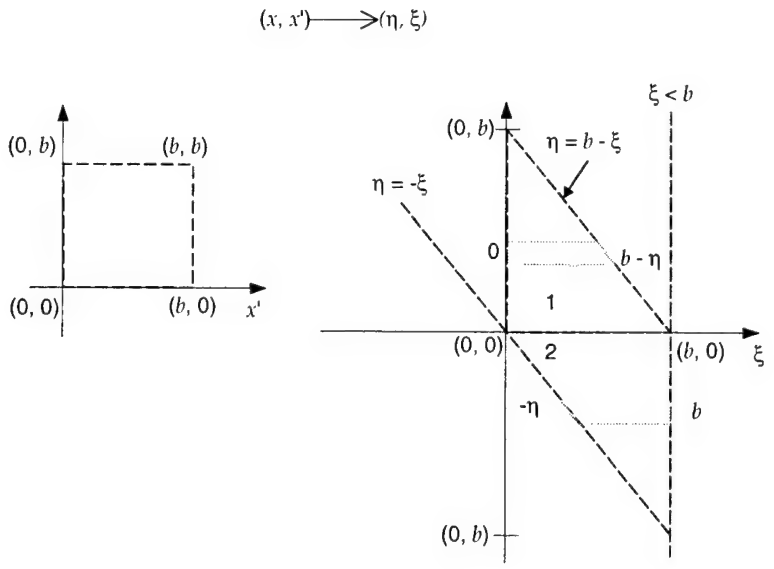

Figure B-3. Transformation of parameter space for Green's function type integrals.

space impedance, equation (B-31) can be written

$$\frac{Y_{\text{in}}}{Y_{H0}} = \frac{\xi_0 \omega \varepsilon_0}{k_{z0}^2 b} \left\{ k_{z0} b \int_0^{k_{z0}b} H_0^{(2)}(\eta)\, d\eta - \int_0^{k_{z0}b} \eta H_0^{(2)}(\eta)\, d\eta \right\} . \qquad \text{(B-34)}$$

For cylindrical Bessel functions, $Z_\nu(\zeta)$, we know that $\int \zeta Z_\nu(\zeta) d\zeta = \zeta Z_{\nu+1}(\zeta)$ and so

$$\int_0^{k_{z0}b} \frac{\zeta}{k_{z0}b} Z_\nu(\zeta)\, d\zeta = \frac{\zeta}{k_{z0}b} Z_{\nu+1}(\zeta) \Big|_0^{k_{z0}b} = Z_{\nu+1}(k_{z0}b) - \lim_{\zeta \to 0} \left(\frac{\zeta Z_{\nu+1}(\zeta)}{k_{z0}b} \right) . \qquad \text{(B-35)}$$

Then using equation (B-35) to simplify the second term in equation (B-34), we find

$$\frac{Y_{\text{in}}}{Y_{H0}} = \frac{\xi_0 \omega \varepsilon_0}{k_{z0}} \left\{ \int_0^{k_{z0}b} H_0^{(2)}(\eta)\, d\eta - H_1^{(2)}(k_{z0}b) + \lim_{\eta \to 0} \left(\frac{\eta H_1^{(2)}(\eta)}{k_{z0}b} \right) \right\} . \qquad \text{(B-36a)}$$

Where we use

$$\lim_{\eta \to 0} \left(\frac{\eta H_1^{(2)}(\eta)}{k_{z0}b} \right) = \frac{2j}{\pi k_{z0}b} . \qquad \text{(B-36b)}$$

The normalized input admittance, y_{in}, for the parallel plate guide radiating into a half-space is thus from equation (B-36a) with equation (B-36b)

$$y_{\text{in}} = \int_0^{k_{z0}b} H_0^{(2)}(\eta) d\eta - H_1^{(2)}(k_{z0}b) + j \frac{2}{\pi k_{z0}b} . \qquad \text{(B-37)}$$

Expanding the Hankel functions into Bessel and Neumann functions, $H_\nu^{(2)}(\zeta) = J_\nu(\zeta) - jN_\nu(\zeta)$, equation (B-37) is written in terms of the input conductance and susceptance, normalized to the H-type mode admittance

$$g_{\text{in}} = \frac{G}{Y_{H0}} = \int_0^{k_{z0}b} J_0(\eta) d\eta - J_1(k_{z0}b) \qquad \text{(B-38a)}$$

$$b_{\text{in}} = \frac{B}{Y_{H0}} = -\int_0^{k_{z0}b} N_0(\eta)d\eta + N_1(k_{z0}b) + \frac{2}{\pi k_{z0}b} . \qquad \text{(B-38b)}$$

It is important to note that the expression (B-38b) in *The Waveguide Handbook* includes a sign error in the first term [3, p 184, equation (2a)]. Now when the aperture is not the full waveguide width, $d < b$, then the variational expression can still be used to obtain equivalent circuit parameters. The rationale for this approach is that with constant aperture field, the equivalent circuit depends only on the external field. This can be seen from the variational expression (B-29) where the first term that depends on the internal fields vanishes when E_{xA} is constant. Then for a narrow aperture, the equivalent circuit parameters are given by equation (B-38) with b replaced by d.

The normalized circuit parameters in equation (B-38) represent the "exact" solution as obtained by the variational method. A closed form approximation can be obtained with the small argument formulas for the Bessel functions. From the series representations, we have

$$\mathbf{J}_0(z) = 1 + O\left(z^2\right), \quad \text{and } \mathbf{N}_0(z) = -\frac{2}{\pi}\ln\left(\frac{gz}{2}\right) + O\left(z^2\right) \qquad \text{(B-39a)}$$

$$\mathbf{J}_1(z) = \frac{z}{2} + O\left(z^2\right), \quad \text{and } \mathbf{N}_1(z) = -\frac{1}{\pi}\left(\frac{z}{2}\right)^{-1} + \frac{z}{\pi}\ln\left(\frac{z}{2}\right) + \frac{z}{\pi}\left(\text{lng} - \frac{1}{2}\right) + O\left(z^2\right) \qquad \text{(B-39b)}$$

in which $g = e^c = 1.781...$, with the irrational number $c = 0.577...$ being Euler's constant. Thus, when $k_{z0}d < 1$, equation (B-38a) becomes (with b replaced by d)

$$g_{\text{in}} \approx \int_0^{k_{z0}d} d\eta - \frac{k_{z0}d}{2} = \frac{k_{z0}d}{2} . \qquad \text{(B-40)}$$

This small argument approximation for the equivalent conductance is the same as the static result provided by Marcuvitz [3, p 184, equation (1b)]. The equivalent susceptance from equation (B-38b) becomes (with b replaced by d)

$$b_{\text{in}} \approx -\frac{2}{\pi}\int_0^{k_{z0}d} \ln\left(\frac{g\eta}{2}\right)d\eta + \frac{k_{z0}d}{\pi}\ln\left(\frac{k_{z0}d}{2}\right) + \frac{k_{z0}d}{\pi}\ln\left(g - \frac{1}{2}\right) . \qquad \text{(B-41)}$$

Integrating and simplifying, we get

$$b_{\text{in}} \approx \frac{k_{z0}d}{\pi}\ln\left(\frac{2\text{e}\sqrt{\text{e}}}{gk_{z0}d}\right) \qquad \text{(B-42)}$$

in which the irrational number e = 2.71828... is the base of the natural logarithm. On the other hand, Marcuvitz gives the static solution for the susceptance as [3, p 184, equation (2b)]

$$b_{\text{in}} \approx \frac{k_{z0}d}{\pi}\ln\left(\frac{\text{e}\pi}{gk_{z0}d}\right) \qquad \text{(B-43)}$$

which cannot be obtained from the truncated series representation of the Neumann functions. A comparison of the variational result for the susceptibility equation (B-38b) to the static result equation (B-43) and the small argument approximation (B-42) is provided in figure B-4. The small argument approximation equation (B-42) is closer to the variational result for $k_{z0}d < 0.5$. For larger $k_{z0}d$, the static result is a better approximation than equation (B-42) although the difference is negligible for $k_{z0}d < 1$, our case of interest. Then equation (B-43) is used when a closed form approximation is required; otherwise, the "exact" susceptance is calculated numerically from equation (B-38b).

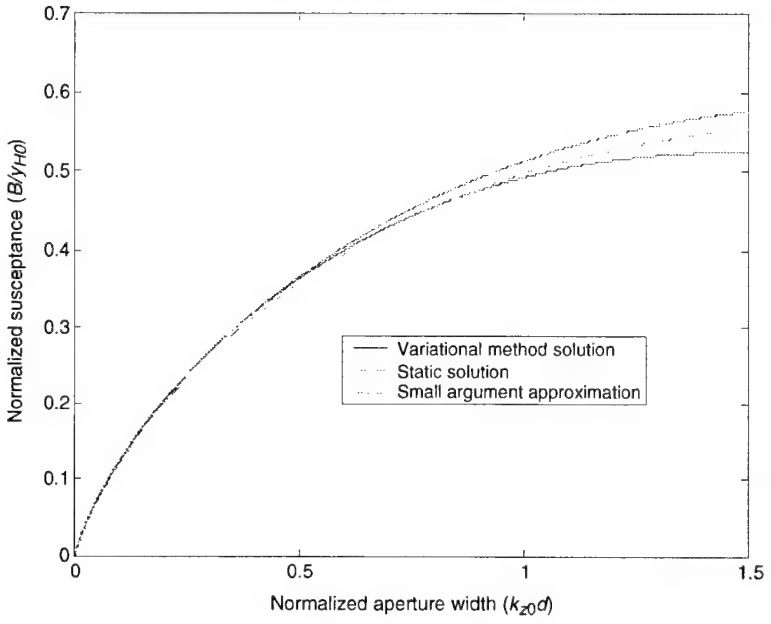

Figure B-4. Normalized susceptance for a parallel plate fed aperture radiating into a half-space.

Appendix C. The Transverse Resonance Method

The electromagnetic (EM) fields within a hollow rectangular waveguide are represented as an infinite number of modes that are propagating or attenuating along the guide. The EM field of each mode can be factored into transverse and longitudinal field components with respect to the direction of propagation allowing a transmission line description for each mode. Even with discontinuities, a waveguide can then be completely described by an infinite number of transmission lines [3, p 6]. Following Marcuvitz, we first summarize the conventional (i.e., transverse to y) mode decomposition for the rectangular waveguide shown in figure C-1 with boundary surface S in the cross-sectional plane. Next, we consider modes transverse to z with the H-type mode decomposition derived in appendix A. We place the origin as shown in figure C-1 so that a transverse transmission line analysis in the cross-sectional plane corresponds to propagation along the positive z-axis. We describe the transverse resonance method by applying the technique to the closed waveguide. We then apply the method to a localized waveguide discontinuity such as a zero-thickness aperture in the waveguide narrow wall.

C.1 Rectangular Waveguide Modes

We only consider transverse electric (TE) or H-modes, characterized by modal fields with $E_y = 0$ while H_y must satisfy a wave equation for propagating or attenuating waves along the y-direction with longitudinal propagation constant $\gamma = j\beta$. When completely filled with a uniform dielectric material having permittivity, $\epsilon = \epsilon_0\epsilon_r$, and permeability, $\mu = \mu_0\mu_r$, the modal structure is the same as for the air-filled waveguide but with a different guide wavelength and characteristic impedance. Referring to figure C-1, take the xz-plane as the transverse plane and define the transverse

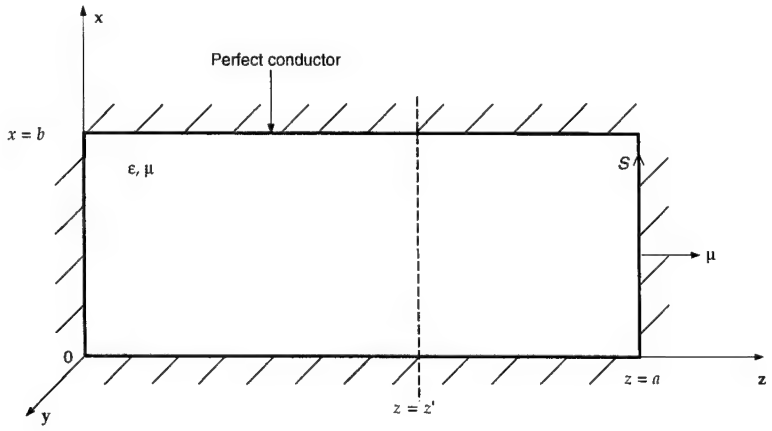

Figure C-1. Hollow rectangular waveguide (with perfect condctor walls) filled with a uniform material.

(to y) Del operator, $\nabla_{ty} \equiv \frac{\partial}{\partial x}\hat{\mathbf{x}} + \frac{\partial}{\partial z}\hat{\mathbf{z}}$. Then, from the Maxwell field equations, the EM fields must satisfy

$$-\frac{\partial \mathbf{E}_{ty}}{\partial y} = j\omega\mu \left[\bar{\bar{\mathbf{I}}} + \frac{\nabla_{ty}\nabla_{ty}}{k^2}\right] \cdot (\mathbf{H}_{ty} \times \hat{\mathbf{y}}) \ , \quad \text{and} \tag{C-1a}$$

$$-\frac{\partial \mathbf{H}_{ty}}{\partial y} = j\omega\varepsilon \left[\bar{\bar{\mathbf{I}}} + \frac{\nabla_{ty}\nabla_{ty}}{k^2}\right] \cdot (\hat{\mathbf{y}} \times \mathbf{E}_{ty}) \tag{C-1b}$$

in which $\bar{\bar{\mathbf{I}}} = \hat{\mathbf{x}}\hat{\mathbf{x}} + \hat{\mathbf{y}}\hat{\mathbf{y}} + \hat{\mathbf{z}}\hat{\mathbf{z}}$ is the unit dyadic. The longitudinal fields are

$$j\omega\mu H_y = \nabla_{ty} \cdot (\hat{\mathbf{y}} \times \mathbf{E}_{ty}) \ , \quad \text{and} \tag{C-2a}$$

$$j\omega\varepsilon E_y = \nabla_{ty} \cdot (\mathbf{H}_{ty} \times \hat{\mathbf{y}}) \tag{C-2b}$$

This representation is equivalent to the Maxwell equations but allows separation of the transverse and longitudinal field variation [3, p 4]. In the spirit of separation of variables, expand the transverse (to y) fields in vector modal functions that are constructed to have the correct x and z spatial variation for each mode i,

$$\mathbf{E}_{ty}(x, y, z) = V_i(y)\mathbf{e}_i(x, z) \ , \quad \text{and} \tag{C-3a}$$

$$\mathbf{H}_{ty}(x, y, z) = I_i(y)\mathbf{h}_i(x, z) \tag{C-3b}$$

in which i denotes a double index mn. The vector functions define the cross-sectional form of the mode fields while the voltage and current functions are the root mean square (rms) amplitudes of the transverse EM fields at any point y along the propagation direction. Without discontinuities, substituting equation (C-3) into equation (C-1) results in an infinite set of transmission line equations

$$-\frac{dV_{mn}(y)}{dy} = jk_{ymn}Z_{mn}I_{mn}(y) \ , \quad \text{and} \tag{C-4a}$$

$$-\frac{dI_{mn}(y)}{dy} = jk_{ymn}Y_{mn}V_{mn}(y) \tag{C-4b}$$

which define the longitudinal variation of the mode amplitudes. Each mnth-mode corresponds to a transmission line with $Z_{mn} = 1/Y_{mn}$ the characteristic (wave) impedance and jk_{ymn} the propagation constant along y. When we use equation (C-3) in equation (C-1) and take account of equation (C-4), the transverse (to y) mode functions are

$$\mathbf{e}_{mn} = \frac{\omega\mu}{k_{ymn}Z_{mn}} \left[\bar{\bar{\mathbf{I}}} + \frac{\nabla_{ty}\nabla_{ty}}{k^2}\right] \cdot (\mathbf{h}_{mn} \times \hat{\mathbf{y}}) \ , \quad \text{and} \tag{C-5a}$$

$$\mathbf{h}_{mn} = \frac{\omega\varepsilon}{k_{ymn}Y_{mn}} \left[\bar{\bar{\mathbf{I}}} + \frac{\nabla_{ty}\nabla_{ty}}{k^2}\right] \cdot (\hat{\mathbf{y}} \times \mathbf{e}_{mn}) \ . \tag{C-5b}$$

The transverse EM fields are then obtained from equation (C-3) in terms of the transmission line voltage and current functions. With equation (C-3) in equation (C-2), the "longitudinal" field components are

$$j\omega\mu H_y = V_{mn}(y)\nabla_{ty} \cdot (\hat{\mathbf{y}} \times \mathbf{e}_{mn}) \ , \quad \text{and} \tag{C-6a}$$

$$j\omega\varepsilon E_y = I_{mn}(y)\nabla_{ty}\cdot(\mathbf{h}_{mn}\times\hat{\mathbf{y}})\ . \qquad \text{(C-6b)}$$

With $\mathbf{h}_{mn} = \hat{\mathbf{y}}\times\mathbf{e}_{mn}$ and $\mathbf{e}_{mn} = \hat{\mathbf{y}}\times\nabla_{ty}\psi_{mn}$, the classical TE-modal decomposition is obtained in terms of vector modes derivable from a scalar mode function. The mode function satisfies the scalar wave equation, $\left(\nabla_{ty}^2 + k_{tmn}^2\right)\psi_{mn}(x,z) = 0$ subject to the boundary condition $\frac{\partial\psi_{mn}}{\partial\nu} = 0$, on S for unit outward normal vector ν. Suitable vector modal functions, chosen to be orthonormal over the waveguide cross section,

$$\int_0^a\int_0^b \mathbf{e}_{mn}\bullet\,\mathbf{e}_{pq}^*\,dxdz = \delta_{np}\delta_{mq} = \begin{cases}1 & \text{for } n=p \quad \text{and } m=q\\ 0 & \text{otherwise}\end{cases} \qquad \text{(C-6c)}$$

for all m =1, 2,... and n = 0, 1, 2,..., allow the cross-sectional dependence to be eliminated from equation (C-1). The H-mode functions, $\mathbf{e}_{mn}$, normalized over the waveguide cross section are then derivable from the scalar function

$$\psi_{mn}(x,z) = \frac{\sqrt{\xi_m\xi_n}A_{mn}\cos\left(\frac{n\pi x}{b}\right)\cos\left(\frac{m\pi z}{a}\right)}{\pi\sqrt{\frac{m^2b}{a}+\frac{n^2d}{b}}}, m=1,2,\ldots \quad \text{and } n=0,1,2,\ldots$$

$$\text{with } \xi_m = \begin{cases}1 & m=0\\ 2 & m\neq 0\end{cases} \quad \text{and } \xi_n = \begin{cases}1 & n=0\\ 2 & n\neq 0\end{cases} \qquad \text{(C-7)}$$

in which A_{mn} is the mnth-mode amplitude normalization factor and the time dependence, $e^{j\omega t}$, is suppressed. The wavenumber corresponding to the angular frequency, ω is written in terms of longitudinal and transverse components, $k^2 = \beta^2 + k_{tmn}^2$. Then the mode function satisfies the scalar wave (Helmholtz) equation with "cutoff" or transverse wave number

$$k_{tmn}^2 = k^2 - \beta^2 = \left(\frac{m\pi}{a}\right)^2 + \left(\frac{n\pi}{b}\right)^2 \qquad \text{(C-8)}$$

for the mnth-mode. When we use equation (C-7) in equation (C-5), we find the vector mode functions are

$$\mathbf{e}_{mn}(x,z) = \hat{\mathbf{y}}\times\nabla_{ty}\psi_{mn} = -\frac{\sqrt{\xi_m\xi_n}A_{mn}}{\pi\sqrt{\frac{m^2b}{a}+\frac{n^2a}{b}}}\left\{\frac{m\pi}{a}\sin\left(\frac{m\pi z}{a}\right)\hat{\mathbf{x}} - \frac{n\pi}{b}\sin\left(\frac{n\pi x}{b}\right)\hat{\mathbf{z}}\right\}\ , \quad \text{and} \qquad \text{(C-9a)}$$

$$\mathbf{h}_{mn}(x,z) = \hat{\mathbf{y}}\times\mathbf{e}_{mn} = \frac{\sqrt{\xi_m\xi_n}A_{mn}}{\pi\sqrt{\frac{m^2b}{a}+\frac{n^2a}{b}}}\left\{\frac{n\pi}{b}\sin\left(\frac{n\pi x}{b}\right)\hat{\mathbf{x}} + \frac{m\pi}{a}\sin\left(\frac{m\pi z}{a}\right)\hat{\mathbf{z}}\right\}\ . \qquad \text{(C-9b)}$$

The H-field can be written in terms of the (transverse) mode function equation (C-7) as

$$\mathbf{H}_{mn} = \frac{j\beta Z_0}{j\omega\mu}I_{mn}(y)\mathbf{h}_{mn}(x,z) + \hat{\mathbf{y}}\frac{V_{mn}(y)}{j\omega\mu}\nabla_{ty}^2\psi_{mn}(x,z) \qquad \text{(C-10)}$$

and ψ_{mn} satisfies the scalar wave equation, so the EM fields are

$$\mathbf{H}_{mn} = \frac{\beta Z_0}{\omega\mu} I_{mn}(y)\mathbf{h}_{mn}(x,z) + \hat{\mathbf{y}}\frac{V_{mn}(y)}{j\omega\mu} k_{tmn}^2 \psi_{mn}(x,z)\,, \quad \text{and} \tag{C-11a}$$

$$\mathbf{E}_{mn}(x,y,z) = V_{mn}(y)\mathbf{e}_{mn}(x,z) \tag{C-11b}$$

where the characteristic impedance is the ratio of the voltage to current at any terminal plane. We also know that the transverse field components propagate down the guide as plane waves. Then for propagation along y we must have

$$\hat{\mathbf{y}} \times \mathbf{E}_{mn} = Z_0 \mathbf{H}_{mn}, \quad \text{so } Z_0 = \frac{E_z}{H_x} = -\frac{E_x}{H_z}\,. \tag{C-12}$$

Then from equation (C-11), we see that $Z_0 = \omega\mu/\beta$ is the waveguide characteristic (wave) impedance for H-modes. The EM fields are thus expressed in terms of completely transverse vector mode functions and longitudinal modal "transmission line" voltage and current amplitudes. The voltage and current mode amplitudes defined by equation (C-4) satisfy the one-dimensional wave equation so are either propagating or attenuating waves along y. For propagating waves, an impedance description using standing waves or a scattering description using traveling waves can be used to represent the voltage and current mode amplitudes leading to a complete description of the modal fields [3, p 9–13].

For the special case when $m = 1$ and $n = 0$ (i.e., the H_{10}-mode), the fundamental (or principal) mode EM fields from equation (C-11) simplify to

$$\mathbf{E}_{10} = -A_{10}V_{10}(y)\sqrt{\frac{2}{ab}}\sin\left(\frac{\pi z}{a}\right)e^{-j\beta y}\hat{\mathbf{x}}\,, \quad \text{and} \tag{C-13a}$$

$$\mathbf{H}_{10} = A_{10}\sqrt{\frac{2}{ab}}\left\{\frac{k_{t10}^2}{j\omega\mu}V_{10}(y)\cos\left(\frac{\pi z}{a}\right)\hat{\mathbf{y}} + I_{10}(y)\sin\left(\frac{\pi z}{a}\right)\hat{\mathbf{z}}\right\}e^{-j\beta y}\,. \tag{C-13b}$$

We assume that only the fundamental mode propagates so that from equation (C-8) the transverse wavenumber is $k_{t10} = \pi/a$. For average or rms field quantities, power flow is given by the Poynting vector, $\mathbf{P_{10}} = \mathrm{Re}\,(\mathbf{E_{10}} \times \mathbf{H_{10}^*})$. The cross product from equation (C-13) is

$$\mathbf{E}_{10} \times \mathbf{H}_{10}^* = |A_{10}|^2\left(\frac{2}{ab}\right)\left\{V_{10}(y)I_{10}^*(y)\sin^2\left(\frac{\pi z}{a}\right)\hat{\mathbf{y}} - |V_{10}(y)|^2\left(\frac{\pi}{a}\right)^2\frac{j}{\omega\mu}\sin\left(\frac{\pi z}{a}\right)\cos\left(\frac{\pi z}{a}\right)\hat{\mathbf{z}}\right\}\,. \tag{C-14}$$

The mode amplitude is determined in terms of the power flowing at some point y' within the guide. The input power $\mathbf{P}_{\mathrm{in}}(y')$, at some reference plane y' is $\mathbf{P}_{10}(x',y',z')$ integrated over the waveguide cross section. Since equation (C-14) is independent of x, we have

$$\mathbf{P}_{\mathrm{in}}(y') \equiv b\int_0^a \mathbf{P}_{10}(y',z')dz' = |A_{10}|^2\,\mathrm{Re}\,(V_{10}(y')I_{10}^*(y'))\,\hat{\mathbf{y}}\,. \tag{C-15}$$

The fundamental mode amplitude is evidently then the normalization required to have $|\mathbf{P}_{\text{in}}(y')| = \text{Re}(\text{V}_{10}(\text{y}')\text{I}_{10}^*(\text{y}'))$ at some reference plane $y = y'$, so $A_{10} = 1$ is a convenient normalization. The transmission line characterization of the mode is not unique, and different normalization constants could be used [3, p 8]. However, absolute impedance comparisons are typically unnecessary so the mode description can be left in terms of a single amplitude coefficient determined from an appropriate normalization.

We now summarize waveguide modes that are transverse to the z-direction, as developed in appendix A. The vector EM fields $\mathbf{E}_{mp}$ and $\mathbf{H}_{mp}$ are expressed in terms of the mode function,

$$\psi_p(x,y) = A_p \cos\left(\frac{p\pi x}{b}\right) e^{-j\beta y} \tag{C-16}$$

with amplitude normalization factor Ap. This mode function satisfies the scalar wave equation

$$\left(\nabla_{tz}^2 + k_{tp}^2\right)\psi_p(x,y) = 0 \tag{C-17}$$

with transverse (to z) wave number for mode p, $k_{tp}^2 = k^2 - k_{zm}^2$, and $\nabla_{tz} \equiv \hat{\mathbf{x}}\frac{\partial}{\partial x} + \hat{\mathbf{y}}\frac{\partial}{\partial y}$. Now the wavenumber is decomposed into components with respect to the z-direction, or

$$k^2 = k_{tp}^2 + k_{zm}^2 = \beta^2 + \left(\frac{p\pi}{b}\right)^2 + k_{zm}^2 \,. \tag{C-18}$$

The propagation constant in the transverse direction, k_{zm}, is unknown but can be found via the transverse resonance technique by defining voltage, $V_p(z)$ and current, $I_p(z)$ mode amplitudes for the z-directed transmission line. These functions satisfy transmission line equations for propagation in the transverse direction, or

$$-\frac{dV_p(z)}{dz} = jk_{zm}Z_{Hp}I_p(z)\,, \quad \text{and} \tag{C-19a}$$

$$-\frac{dI_p(z)}{dz} = jk_{zm}Y_{Hp}V_p(z) \tag{C-19b}$$

where the characteristic impedance for the pth-mode is from appendix A

$$Z_{Hp} = \frac{k_{zm}\omega\mu}{k^2 - \beta^2} \,. \tag{C-20}$$

The vector mode functions for the closed waveguide are H-type modes (see app A)

$$\mathbf{h}_p(x,y) = -\nabla_{tz}\psi_p(x,y)\,, \quad \text{and} \tag{C-21a}$$

$$\mathbf{e}_p(x,y) = \mathbf{h}_p(x,y) \times \hat{\mathbf{z}} \,. \tag{C-21b}$$

Compared to equation (C-2) for standard H-modes propagating along y, equation (C-21) yields hybrid modes in this direction. The vector EM fields are

$$\mathbf{E}_{mp} = V_p(z)\mathbf{e}_p(x,y)\,, \quad \text{and} \tag{C-22a}$$

$$\mathbf{H}_{mp} = I_p(z)\mathbf{h}_p(x,y) + \hat{\mathbf{z}}\frac{\nabla_{tz}\cdot(\hat{\mathbf{z}}\times\mathbf{E}_{mp})}{j\omega\mu} = I_p(z)\mathbf{h}_p(x,y) + \hat{\mathbf{z}}\frac{k_{tp}^2}{j\omega\mu}\psi_p(x,y)V_p(z) \tag{C-22b}$$

where the amplitudes $V_p(z)$ and $I_p(z)$ can be found for the pth-mode in terms of the voltage and current amplitude at a single point [3, p 9].

C.2 Uniform Waveguide

The closed waveguide in the transverse direction can be considered as the junction of two shorted transmission lines as shown in figure C-2. For now, let both lines have the same characteristic impedance $Z_0 = Z_{Hp}$, and propagation constant $\gamma_z = jk_{zm}$. The transverse resonance condition requires that at resonance the input impedance (or admittance) "looking" in each direction must sum to zero at any point $0 \le z\prime \le a$ [4, p 167]. That is

$$\overleftarrow{Z}_{\text{in}}(z') + \vec{Z}_{\text{in}}(z') = 0, \quad \text{when } 0 \le z' \le a, \quad \text{or} \tag{C-23a}$$

$$\overleftarrow{Y}_{\text{in}}(z') + \vec{Y}_{\text{in}}(z') = 0, \quad \text{when } 0 \le z' \le a \tag{C-23b}$$

where the arrows denote the impedance (or admittance) in the decreasing or increasing z-direction, respectively. At a point, z' located a distance l from the load impedance, $Z_l(l)$, the input inpedance for purely imaginary propagation constant reduces to the well-known expression

$$Z_{\text{in}}(z') \equiv Z(z') = Z_0\frac{Z_l(l) + jZ_0\tan(k_{zm}l)}{Z_0 + jZ_l(l)\tan(k_{zm}l)} \tag{C-24}$$

where the load impedance and distance to the load on the left or the right of z' are to be used, for the input impedance looking to the left or right, respectively. For $z' = 0$, we have $l = 0$ so with $Z_l(0) = 0$, we see from equation (C-24) that the impedance looking to the left vanishes. Looking to the right, the termination is also a short circuit or $Z_l(a) = 0$, with $l = a - z' = a$. Then using equation (C-24) with $Z_0 = Z_{Hp}$ in equation (C-23a), we find the resonance condition is simply

$$\vec{Z}_{\text{in}}(0) = jZ_{Hp}\tan(k_{zm}a) = 0 \tag{C-25}$$

which requires that $k_{zm} = (m\pi/a)$. Thus, the transverse resonance method applied to a uniform, closed waveguide (equivalent to a transmission line with shorted terminals at $z = 0$ and $z = a$) yields $k_{zm} = (m\pi/a)$ as expected.

Figure C-2. Waveguide transverse transmission line description as a junction of two shorted lines.

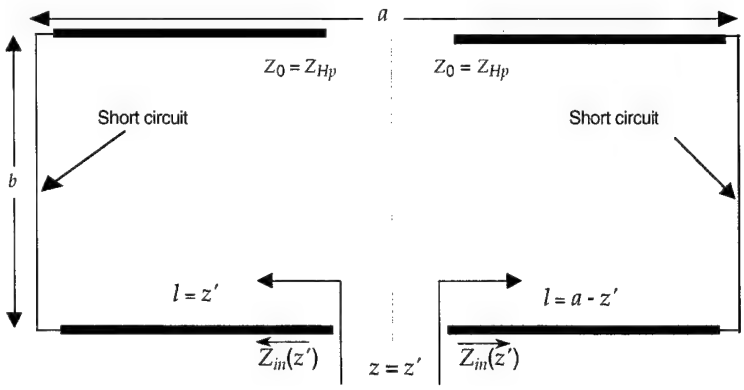

For the closed rectangular waveguide, the wavenumber magnitude from equation (C-18) is then

$$k = \sqrt{k_{tp}^2 + k_{zm}^2} = \sqrt{\beta^2 + \left(\frac{p\pi}{b}\right)^2 + \left(\frac{m\pi}{a}\right)^2}\,. \tag{C-26}$$

So with an H-type mode decomposition, the transverse resonance condition results in the H_{mn}-mode waveguide fields, as expected. The H-type hybrid mode fields may also be of interest, and we show that the fundamental H-type mode reduces to the H_{10}-mode. The magnetic vector mode function from equation (C-21a) is

$$\mathbf{h}_p(x,y) = -A_p \nabla_{tz} \left(\cos\left[\frac{p\pi x}{b}\right] \mathrm{e}^{-j\beta y} \right) = A_p \left\{ \left(\frac{p\pi}{b}\right) \sin\left(\frac{p\pi x}{b}\right) \hat{\mathbf{x}} + j\beta \cos\left(\frac{p\pi x}{b}\right) \hat{\mathbf{y}} \right\} e^{-j\beta y}\,. \tag{C-27}$$

Then using this in equation (C-21b), we find

$$\mathbf{e}_p(x,y) = \mathbf{h}_p(x,y) \times \hat{\mathbf{z}} = A_p \left\{ j\beta \cos\left(\frac{p\pi x}{b}\right) \hat{\mathbf{x}} - \frac{p\pi}{b} \sin\left(\frac{p\pi x}{b}\right) \hat{\mathbf{y}} \right\} e^{-j\beta y} \tag{C-28}$$

which has both x- and y-components. Compared to the standard TE-TM mode decomposition, these functions represent hybrid modes having both E_y and H_y fields in the longitudinal (y-) direction. In the special case of $p = 0$, equation (C-28) becomes

$$\mathbf{e}_0(x,y) = A_0 j\beta e^{-j\beta y} \hat{\mathbf{x}}\,. \tag{C-29}$$

For a shorted transmission line, the voltage must vanish at each end so a Fourier sine series could represent the transverse voltage

$$V_p(z) = \sum_{m=1}^{\infty} B_{mp} \sin\left(\frac{m\pi z}{a}\right)\,. \tag{C-30}$$

The sum is over a possibly infinite number of modes, each with amplitude B_{mp}, a complex constant. From the transmission line equation (C-19a), we have

$$I_p(z) = -\frac{dV_p(z)}{dz} \frac{1}{jZ_{Hp}k_{zm}} = -\frac{k^2 - \beta^2}{k_{zm}\omega\mu} \frac{dV_p(z)}{dz} \frac{1}{jk_{zm}} = j\frac{k^2 - \beta^2}{k_{zm}^2\omega\mu} \frac{dV_p(z)}{dz} \tag{C-31}$$

so that the pth-mode current is

$$I_p(z) = j\frac{k^2-\beta^2}{\omega\mu}\sum_{m=1}^{\infty}\left(\frac{m\pi}{k_{zm}^2 a}\right)B_{mp}\cos\left(\frac{m\pi z}{a}\right). \tag{C-32}$$

The EM fields can now be found and for the case $p = 0$ the E-field is

$$\mathbf{E}_{m0} = j\beta e^{-j\beta y}\sum_{m=1}^{\infty}B_{m0}\sin\left(\frac{m\pi z}{a}\right)\hat{\mathbf{x}}\,. \tag{C-33}$$

The normalization constant A_0 is absorbed in the mode amplitude B_{m0}. The H-field when $p = 0$ is

$$\mathbf{H}_{m0} = -\left\{\frac{\beta}{\omega\mu}\sum_{m=1}^{\infty}\left(\frac{m\pi}{a}\right)B_{m0}\cos\left(\frac{m\pi z}{a}\right)\hat{\mathbf{y}} + \frac{j\beta^2}{\omega\mu}\sum_{m=1}^{\infty}B_{m0}\sin\left(\frac{m\pi z}{a}\right)\hat{\mathbf{z}}\right\}e^{-j\beta y}\,. \tag{C-34}$$

Then for the typical case of interest $m = 1$, the waveguide fields are

$$\mathbf{E}_{10} = j\beta e^{-j\beta y}B_{10}\sin\left(\frac{\pi z}{a}\right)\hat{\mathbf{x}}\,, \quad \text{and} \tag{C-35a}$$

$$\mathbf{H}_{10} = -B_{10}\left\{\frac{\pi}{a}\left(\frac{\beta}{\omega\mu}\right)\cos\left(\frac{\pi z}{a}\right)\hat{\mathbf{y}} + \frac{j\beta^2}{\omega\mu}\sin\left(\frac{\pi z}{a}\right)\hat{\mathbf{z}}\right\}e^{-j\beta y}\,. \tag{C-35b}$$

These H-type fields differ from the H_{10}-mode fields equation (C-13) by a complex constant. The amplitude, B_{10} is determined by requiring that the average power, $\mathbf{P}_{10} = \mathrm{Re}(\mathbf{E}_{10}\times(\mathbf{H}_{10}^*)$, integrated across the waveguide is the input power, $P_{\mathrm{in}}(y')$. The cross product from equation (C-35) is

$$\mathbf{E}_{10}\times\mathbf{H}_{10}^* = \left(\frac{\beta^3}{\omega\mu}\right)|B_{10}|^2\sin^2\left(\frac{\pi z}{a}\right)\hat{\mathbf{y}} + \left(\frac{\beta^2}{\omega\mu}\right)\frac{\pi}{a}|B_{10}|^2\sin\left(\frac{\pi z}{a}\right)\cos\left(\frac{\pi z}{a}\right)\hat{\mathbf{z}} \tag{C-36}$$

which is purely real and independent of x, and with $k_{t0} = \beta$ from equation (C-26) we have

$$\mathbf{P}_{\mathrm{in}}(y') = b\int_0^a \mathbf{P}_{10}dz = \left(\frac{b\beta^3}{\omega\mu}\right)\frac{a}{2}|B_{10}|^2\hat{\mathbf{y}} \tag{C-37}$$

The normalization constant is thus $B_{10} = \sqrt{\frac{2}{ab}}\sqrt{\frac{\omega\mu}{\beta^3}}$, so from equation (C-35) the EM fields are

$$\mathbf{E}_{10} = j\sqrt{\frac{2}{ab}}\sqrt{\frac{\omega\mu}{\beta}}e^{-j\beta y}\sin\left(\frac{\pi z}{a}\right)\hat{\mathbf{x}}\,, \quad \text{and} \tag{C-38a}$$

$$\mathbf{H}_{10} = -\sqrt{\frac{2}{ab}}\sqrt{\frac{\beta}{\omega\mu}}\left\{\left(\frac{\pi}{\beta a}\right)\cos\left(\frac{\pi z}{a}\right)\hat{\mathbf{y}} + j\sin\left(\frac{\pi z}{a}\right)\hat{\mathbf{z}}\right\}\mathrm{e}^{-j\beta y}\,. \tag{C-38b}$$

In comparison to the H_{10}-mode fields in the previous section, we find that

$$\frac{A_{10}V_{10}(y')}{A_{10}I_{10}(y')} = \frac{-j}{-j}Z_0 = Z_0 \tag{C-39}$$

or the longitudinal voltage and current amplitudes at some point y' are related by the H_{10}-mode impedance Z_0. Thus, the fundamental H-type mode degenerates to the H_{10}-mode.

C.3 Non-uniform Waveguide

The transverse resonance method can also be applied to the more general case of a rectangular waveguide filled with different but uniform materials as shown in figure C-3. The closed waveguide in the transverse direction is now a junction of shorted transmission lines having different propagation constants and characteristic impedance. As for the uniform guide, H-type modes are used for the transverse mode decomposition in each region. The characteristic impedance for the transmission lines along z to the left and right are Z^1_{Hp} and Z^2_{Hp}, with propagation constant $\gamma_{1zm} = jk_{1zm}$ and $\gamma_{2zm} = jk_{2zm}$, respectively. We outline the transverse resonance method applied to the non-uniform waveguide but omit the details as our interest here is in an air-filled waveguide.

The transverse resonance technique that uses modes transverse to the z-axis is used to determine the transverse wavenumber. To the left at a distance $l = a_0$ away, the termination is a short circuit, or $Z_l(0) = 0$, so that the input impedance looking to the left at $z' = a_0$ is

$$\overleftarrow{Z}_{in}(a_0) = Z^1_{Hp}\frac{Z_l(0) + Z^1_{Hp}\tanh(jk_{1zm}a_0)}{Z^1_{Hp} + Z_l(0)\tanh(jk_{1zm}a_0)} = jZ^1_{Hp}\tan(k_{1zm}a_0)\ . \quad \text{(C-40)}$$

The transverse line to the right is also terminated in a short circuit at a distance $l = a - a_0$ away, or $Z_l(a) = 0$. Then the input impedance looking to the right at $z' = a_0$ is

$$\vec{Z}_{\text{in}}(a_0) = Z^2_{Hp}\frac{Z_l(a) + Z^2_{Hp}\tanh(jk_{2zm}(a-a_0))}{Z^2_{Hp} + Z_l(a)\tanh(jk_{2zm}(a-a_0))} = jZ^2_{Hp}\tan(k_{2zm}(a-a_0))\,. \quad \text{(C-41)}$$

When the wavenumbers are purely real, the resonance condition at $z' = a_0$ requires

$$jZ^1_{Hp}\tan(k_{1zm}a_0) + jZ^2_{Hp}\tan(k_{2zm}(a-a_0)) = 0\,. \quad \text{(C-42)}$$

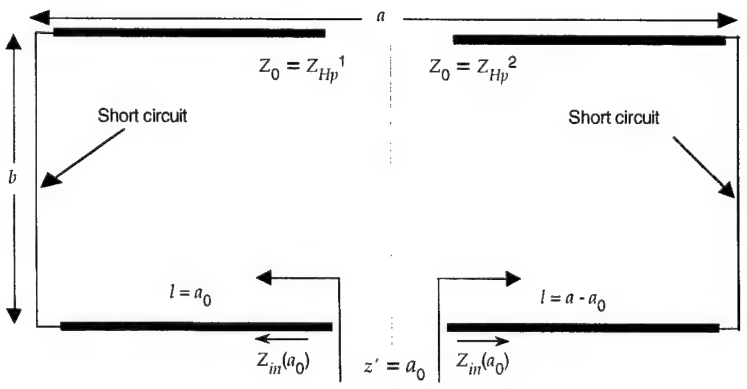

Figure C-3. A closed waveguide transverse description as a junction of different transmission lines.

This transcendental equation is typically written in terms of dimensionless variables since the wavenumber in one region can be written in terms of the other. One equation for the two unknown propagation constants is obtained by subtracting the wavenumber in each region. Applying the transverse resonance condition equation (C-23a) at the material interface, $z' = a_0$ provides another equation. Simultaneous solution then determines the allowed values of the transverse wavenumber for two possible cases, k_{2zm} purely real and k_{2zm} purely imaginary, which are treated separately. The corresponding waveguide mth-mode longitudinal phase constant, β, then determines the phase per unit length in the propagation direction which completes the solution.

For the nonuniform line created by geometric changes in the transverse direction, the approach is slightly modified. The discontinuity is lumped at a terminal plane, $z = a_0 + l_1$, and represented by a discontinuity reactance, jX_D as shown in figure C-4. The input impedance looking to the right is then a composite impedance formed by the parallel combination of the discontinuity impedance and the input impedance of the transmission line to the right terminated in load impedance, Z_l. The input impedance, looking to the right at this location, is

$$\vec{Z}_{\text{in}}(a_0 + l_1) = Z_{Hp}^2 \frac{Z_l(a) + Z_{Hp}^2 j \tan\left(k_{2zm}\left(a - a_0 - l_1\right)\right)}{Z_{Hp}^2 + Z_l(a) j \tan\left(k_{2zm}\left(a - a_0 - l_1\right)\right)} . \tag{C-43}$$

Then at $z' = a_0$ the transmission line to the left is terminated with the combined impedance

$$\tilde{Z}_l(a_0 + l_1) = \frac{jX_D \vec{Z}_{\text{in}}(a_0 + l_1)}{jX_D + \vec{Z}_{\text{in}}(a_0 + l_1)} \tag{C-44}$$

which can be readily calculated, given the discontinuity reactance. The transverse resonance condition applied at $z' = a_0$ then proceeds as before with the input impedance to the left unchanged but to the right we have

$$\vec{Z}_{\text{in}}(a_0) = Z_{Hp}^1 \frac{\tilde{Z}_l(a_0 + l_1) + Z_{Hp}^1 j \tan(k_{1zm} l_1)}{Z_{Hp}^1 + \tilde{Z}_l(a_0 + l_1) j \tan(k_{1zm} l_1)} . \tag{C-45}$$

The resonant condition then yields the system of equations to solve for the transverse wavenumber in each region. The details are omitted, but the approach as outlined again demonstrates the versatility of the transverse resonance method.

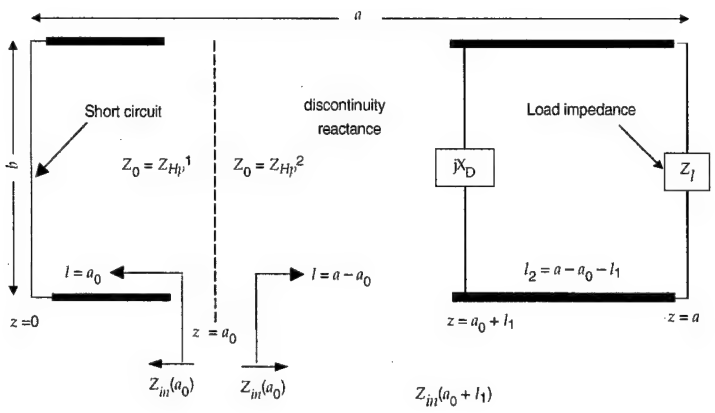

Figure C-4. Waveguide transverse description with a discontinuity represented by a reactance.

C.4 Waveguide Discontinuities

The transverse resonance method can also be applied to the general case of a rectangular waveguide having a localized (i.e., zero thickness) discontinuity in the transverse direction. The discontinuity could be an aperture in the waveguide narrow wall at $z = a$ or any other zero-thickness structure that can be represented by an equivalent circuit. In many cases, the discontinuity is characterized by its admittance, Y_D, that terminates a transmission line with characteristic admittance $Y_0 = Y_{Hp}$ for each of the p possible modes. The transverse resonance condition equation (C-23b) is applied to the input admittance at some point a_0 as shown in figure C-5. The transmission lines could have different parameters but for now, we let $Y_{Hp}^1 = Y_{Hp}^2$, and $\gamma_{1zm} = \gamma_{2zm} = jk_{zm}$, corresponding to a uniform waveguide with a localized discontinuity.

To the left, the termination at distance $l = a_0$ away is a short circuit, or $Y_l(0) = \infty$, so that the input admittance looking to the left at $z' = a_0$ is

$$\overleftarrow{Y}_{\text{in}}(a_0) = Y_{Hp}\frac{Y_l(0) + Y_{Hp}\tanh(jk_{zm}a_0)}{Y_{Hp} + Y_l(0)\tanh(jk_{zm}a_0)} = -jY_{Hp}\cot(k_{zm}a_0)\ . \quad \text{(C-46)}$$

The transverse line to the right is terminated at distance $l = a - a_0$ away in the discontinuity admittance, or $Y_l(a) = Y_D$. Then the input admittance looking to the right at $z' = a_0$ is

$$\vec{Y}_{\text{in}}(a_0) = Y_{Hp}\frac{Y_D + Y_{Hp}j\tan(k_{zm}(a - a_0))}{Y_{Hp} + Y_D j\tan(k_{zm}(a - a_0))}\ . \quad \text{(C-47)}$$

The resonance condition equation (C-23b) applied at $z' = a_0$ requires

$$-jY_{Hp}\cot(k_{zm}a_0) + Y_{Hp}\frac{Y_D + Y_{Hp}j\tan(k_{zm}(a - a_0))}{Y_{Hp} + Y_D j\tan(k_{zm}(a - a_0))} = 0\ . \quad \text{(C-48)}$$

We can calculate the transverse voltage and current functions for mode p by finding the voltage reflection coefficient at $z = a_0$. To the right for mode p

$$V_p(z) = \text{A}\sin[k_{zm}(z - a)] \quad \text{for } a_0 \le z \le a \quad \text{(C-49)}$$

Figure C-5. Waveguide transverse description with a discontinuity represented by a termination admittance.

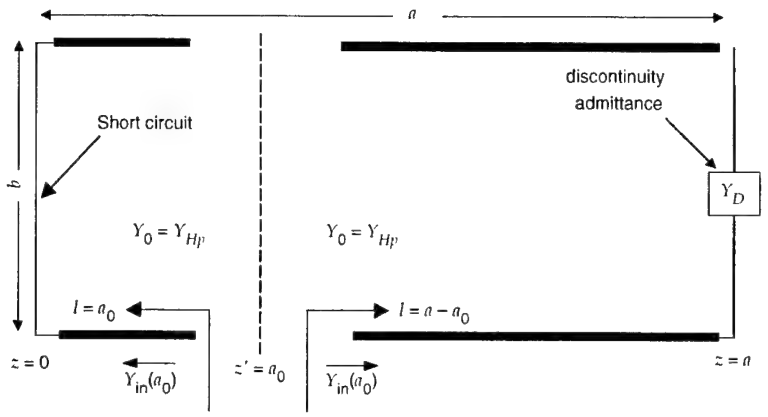

and from the transmission line equation (C-19a) the current modes are

$$I_p(z) = jAY_{Hp}\cos\left[k_{zm}(z-a)\right] \qquad \text{for } a_0 \le z \le a\,. \tag{C-50}$$

The transmission line on the left is terminated at $z = a_0$ with the input admittance looking to the right equation (C-47). The reflection coefficient to the right, for each mode p is then

$$\vec{\Gamma}_p(a_0) = \frac{Y_{Hp} - \vec{Y}_{\text{in}}}{Y_{Hp} + \vec{Y}_{\text{in}}}\,. \tag{C-51}$$

The voltage and current to the left of a_0 include reflected waves from $z = a_0$, or

$$V_p(z) = \mathrm{B}\left[e^{-jk_{zm}(z-a_0)} + \Gamma_p(a_0)\,e^{jk_{zm}(z-a_0)}\right] \quad \text{for } 0 \le z \le a_0 \tag{C-52}$$

since the reference is at $z = a_0$, where $\Gamma_p(a_0)$ is known for each mode. The pth-mode current is

$$I_p(z) = \mathrm{B}Y_{Hp}\left\{e^{-jk_{zm}(z-a_0)} - \Gamma_p(a_0)e^{jk_{zm}(z-a_0)}\right\} \qquad \text{for } 0 \le z \le a_0\,. \tag{C-53}$$

The boundary condition at $z = a_0$ requires continuity of the current and voltage or

$$\mathrm{A}\sin\left[k_{zm}(a_0 - a)\right] - \mathrm{B}\left\{1 + \Gamma(a_0)\right\} = 0\,, \quad \text{and} \tag{C-54}$$

$$j\mathrm{A} - \mathrm{B}\left\{1 - \Gamma(a_0)\right\} = 0\,. \tag{C-55}$$

Nontrivial solutions of this system of equations are possible only if the determinate (det) of coefficients vanishes, or det = 0. This condition has already been satisfied by the transverse resonance condition, and the condition for resonance can be derived by setting det = 0 in the above system. The final result for the voltage and current modes depends on a single constant (the mode amplitude) so let $B = 1$, then from equation (C-55)

$$\mathrm{A} = \frac{1 - \Gamma(a_0)}{j} = j\left(\Gamma(a_0) - 1\right) \tag{C-56}$$

The voltage and current amplitude for each mode p are then determined; thus, the structure of the waveguide fields can be evaluated.

We are interested in the case when $a_0 = a$, with fundamental H-type mode propagation in the transverse (z-) direction or $p = 0$. So for an H_{10}-excited waveguide, we use $m = 1$ and have a reflection coefficient at the plane containing the discontinuity (e.g., an aperture) given by

$$\vec{\Gamma}_0(a) = \frac{Y_{H0} - \vec{Y}_{\text{in}}}{Y_{H0} + \vec{Y}_{\text{in}}} = \frac{Y_{H0} - \frac{Y_D}{Y_{H0}}}{Y_{H0} + \frac{Y_D}{Y_{H0}}} = \frac{Y_{H0} - y_D}{Y_{H0} + y_D} \tag{C-57}$$

in which y_D is the normalized discontinuity admittance. The resonant condition equation (C-48) becomes

$$-j\cot(k_{z1}a) + \frac{Y_D}{Y_{H0}} = 0\,, \quad \text{or} \tag{C-58a}$$

$$k_{z1} = \frac{1}{a}\cot^{-1}(-jy_D) \tag{C-58b}$$

which would require numerical solution. The voltage and current amplitudes to the left are the transverse mode amplitudes throughout the waveguide, or

$$V_0(z) = j\,(\Gamma - 1)\sin\left[k_{z1}\,(z-a)\right]\,, \quad \text{and} \tag{C-59a}$$

$$I_0(z) = (1-\Gamma)\,Y_{H0}\cos\left[k_{z1}(z-a)\right] = (1-\Gamma)\,\frac{k_{z1}}{\omega\mu}\cos\left[k_{z1}(z-a)\right] \tag{C-59b}$$

with $\Gamma = \Gamma_0(a)$ as given by equation (C-57) and $k_{z1} = \sqrt{k^2 - \beta^2}$, given by equation (C-58b). The fundamental mode fields throughout the waveguide with localized discontinuity at $z = a$ are then

$$\mathbf{E}_{10} = A_0(1-\Gamma)\beta\sin\left[k_{z1}(z-a)\right]e^{-j\beta y}\hat{\mathbf{x}}\,, \quad \text{and} \tag{C-60a}$$

$$\mathbf{H}_{10} = A_0\,(1-\Gamma)\,Y_0\left\{jk_{z1}\cos\left[k_{z1}(z-a)\right]\hat{\mathbf{y}} + \beta\sin\left[k_{z1}(z-a)\right]\hat{\mathbf{z}}\right\}e^{-j\beta y} \tag{C-60b}$$

in which $Y_0 = \beta/\omega\mu$ is the H_{10}-mode characteristic admittance and A_0 is the mode amplitude. Of course, these EM fields are perturbed near the discontinuity, but for a "small" discontinuity or at sufficiently large distances, the perturbation would be negligible. This represents the complete solution as obtained by the transverse resonance method for this special case of interest.

Appendix D. Numerical Routines

The numerical calculations presented were accomplished with MATLAB™. The routines as implemented in the form of "m-files" are included for completeness. Minor modifications of these files may be required to produce all the results shown. The subroutine for the FEM calculations is included at the end of the main routine.

```
%%%%%%%%%%%%%%%%%%%%%%%%%%%%%%%%%%%%%%%%%%%%%%%%%%%%%%%%%%%%%%%%%%%%%%%%%%%%%%%%

% NOTAPER.m (CONSTANT WIDTH SLOT)

%%%%%%%%%%%%%%%%%%%%%%%%%%%%%%%%%%%%%%%%%%%%%%%%%%%%%%%%%%%%%%%%%%%%%%%%%%%%%%%%

%FOR PROPAGATION IN WG PERTURBED BY NARROW-WALL SLOT

%COMPUTES COMPLEX PROPAGATION CONSTANT VS. DISTANCE.

%TE10-MODE PROPAGATION IN THE INPUT AND OUTPUT WAVEG-
UIDE

%%%%%%%%%%%%%%%%%%%%%%%%%%%%%%%%%%%%%%%%%%%%%%%%%%%%%%%%%%%%%%%%%%%%%%%%%%%%%%%%

% METHOD OF SOLUTION:

%COMPLEX PROPAGATION CONSTANT BY PERTURBED TRANSVERSE
WAVE

%FOR NARROW SLOTS PERTURB ABOUT SHORT CIRCUIT (see ECE
239 5/2000).

%%%%%%%%%%%%%%%%%%%%%%%%%%%%%%%%%%%%%%%%%%%%%%%%%%%%%%%%%%%%%%%%%%%%%%%%%%%%%%%%

%FEM FOR INPUT REFLECTION (TRANS) COEFF.:

%PROVIDES ANTENNA EFFICIENCY AS 1 - R^2 - T^2 FOR REALIZED
GAIN
```

%%%%%%%%%%%%%%%%%%%%%%%%%%%%%%%%%%%%%%

% REMARKS:

%WAVEGUIDE CROSS-SECTION: a = WIDE DIM. ALONG X,

%HALF-HEIGHT WG: HEIGHT: b = NARROW WALL ALONG Y (E-aperture)

%NARROW-WALL SLOT WIDTH: d ¡¡ b/10; PROPAGATION ALONG Z

%%%%%%%%%%%%%%%%%%%%%%%%%%%%%%%%%%%%%%

% PLOT OUTPUTS:

% 1) SLOT: ALPHA & CURRENT VS NORMALIZED DISTANCE

% 2) PHASE: BETA/BETA10 VS NORMALIZED DISTANCE

% 3) FIELD: FARFIELD PATTERN (H_θ and H_ϕ)

% 4) RADIATION: REALIZED GAIN (H- and E-plane)

%%%%%%%%%%%%%%%%%%%%%%%%%%%%%%%%%%%%%%

% 2) PERTURBATION SOLUTION FOR NARROW SLOTS ONLY

%%%%%%%%%%%%%%%%%%%%%%%%%%%%%%%%%%%%%%

% WOC/27 JULY 2000

%%%%%%%%%%%%%%%%%%%%%%%%%%%%%%%%%%%%%%

tic;

%MM=input('Input number of FEM cells per guide wavelength: ');

MM=100; delta=1e-10;

```
%.....Free space parameters.....

e=exp(1); g=1.781;

mu=4e-7*pi; c=3e8;

%.....Waveguide parameters .....

a=2; b=a/2;

% SET WAVENUMBER FOR OPERATING FREQUENCY

k0=4.25/a; lam=2*pi/k0;

omega=k0*c;

lg10=lam./sqrt(1-(lam/2/a).^2);

beta10=sqrt(k0.^2-(pi/a)^2);

Z10=120*pi*lg10./lam;

%Standard sphereical coordinates theta from z and phi from x

%Current along y-axis with endfire angle theta=phi=pi/2

Nth=200; Nph=100;

thmax=60*pi/180; phmax=pi;

dph=phmax/Nph; dth=thmax/Nth;

th=delta:dth:thmax-delta;

ph=delta:dph:phmax-delta;

%.....Slot parameters .....

'Input uniform slot maximum width :'
```

```
d0=input('normalized to wg height : ');

d0=d0*b;

%%%%%%SLOT LENGTH NORMALIZED TO WG WIDTH

'Input length of slotted section in wavelengths :'

L=input(['Total slot length normalized to wavelength : ']);

L=L*lam;

%%%%%%%%%%%%%%%%%%%%%%%%%%%%%%%%%%%%%%%%%%%%%%%%%%%%%%%%

M=MM*ceil(L/lg10);

N=M+1; dy=L/(N);

y=delta-L/2:dy:L/2;

%%%STEP 1: Uniform slot width vs axial position

d=d0*y./y; dmax = max(d);

%%%STEP 2: Narrow slot width perturbation formulation at each d(y)

G=pi.*d/a/2;

B=(b*log(csc(pi.*d/2/b))+d.*log(a*e/g./d))/a;

A=G.^2+B.^2; R=G./A; X=B./A;

kx0=pi/a + B./A/a + j.*G./A/a;

beta0=sqrt(k0^2-kx0.^2);

%%.....TEST RESULT TO ENSURE NEGATIVE ATTENUATION CONSTANT.....

for mm=1:N;
```

```
if imag(beta0(mm))¿0; beta0(mm)=beta0(mm)-2*i*imag(beta0(mm));

end; end;

alpha=-imag(beta0);

%%%STEP 3: Call FEM code for solution with TE10 at each end

beta0(1)=beta10; beta0(N)=beta10;

%%%%%H-type hybrid mode impedance (see ECE297 3/99)

ZH=omega*mu./real(beta0);

%%%%%%%%%%%%%%%%%%%%%%%%%%%%%%%%%%%%%%%%%%%%%%%%%%%%

[phi]=onedfem(beta0,M,dy,Z10,ZH);

%%%%%%%%%%%%%%%%%%%%%%%%%%%%%%%%%%%%%%%%%%%%%%%%%%%%

%%%STEP 4: CALCULATE REFLECTION, TRANSMISSION & ATTENUATION

RR=((phi(1))-1);

TT=((phi(N))*exp(i*beta0(N)*L));

prad=1 - abs(RR)^2 - abs(TT)^2;,

eff = ceil(prad*100);

%%%STEP 5: CALC AMPLITUDE DISTRIBUTION FROM ALPHA

for mm=1:N;

temp(mm)=alpha(mm); a0=alpha(mm);

F2(mm)=a0*exp(-2*dy*sum(temp));
```

```
end; M0=sqrt(F2);

%%%STEP 6: CALCULATE FAR-FIELD FOR UNIFORM ILLUMINATION
F(y) = 1

for n=1:Nth; for m=1:Nph;

ARG=k0*sin(th(n))*sin(ph(m))-real(beta0);

I2=abs(dy*sum(M0.*exp(i*y.*ARG)))^2;

% Hth2(n,m)=cos(th(n))^2*sin(ph(m))^2*I2;

% Hph2(n,m)=cos(ph(m))^2*I2;

H2(n,m)=cos(th(n))^2*sin(ph(m))^2*I2...

+ cos(ph(m))^2*I2;

end;

%%%%%%%%%%%Factor of four included for integration limits

phiint(n)=dph*sum(H2(n,:))/pi;

end;

denom=dth*sum(phiint.*sin(th));

%%%%%STEP 7: CALCULATE DIRECTIVE GAIN (prad FOR REALIZED
GAIN)

Gp=10*log10(2*L/lam);
['Expected gain (2L/lamda) ',' is ', num2str(Gp,3)]
%%%%PATTERN FROM NUMERICAL INTEGRATION OF CURRENT%%%%

D = prad*H2/denom; clear H2;

G = 10*log10(D); clear D;
```

```
maxG=max(G(:,Nph/2));

for n=1:Nth;

if G(n,Nph/2)==maxG; bw0=n; end; end;

['Integrated peak gain (in dBi) is ', num2str(maxG,4)]

%%%%%%%%%%%%%%%%%%%%%%%%%%%%%%%%%%%%%%%%%%%%%%%%%%%%%%%%

th=th*180/pi; ph=ph*180/pi;

amax = max(alpha/k0);

bmin = min(real(beta0)/beta10);

%%%%.....plot output.....

figure(1);

subplot(2,1,1), plot(y/L,alpha*lam);

axis([-.5 .5 0.8*amax, 1.2*amax]);

text(-.3,1.15*amax,['Slot radiation efficiency = ', num2str(eff),'
text(-.25,1.05*amax,[' k0a = ', num2str(k0*a),' with a = ',num2str(a),' m.']);

text(-.2,0.9*amax,['Total slot length = ', num2str(L/lam,3),' wavelengths.']);

title('Slotted waveguide alpha (in Nepers/wavelength).');

ylabel('Normalized loss (alpha*lamda)')

subplot(2,1,2), plot(y/L,M0/max(M0));

text(-.25,1/2,['Maximum slot width = ', num2str(dmax,3), ' m. ']);

text(.3,1/2,['L = ', num2str(L/a),'a ']);
```

```
title('Current amplitude versus normalized distance.');

xlabel('Normalized distance (y/L)');

ylabel('Normalized current');

figure(4);

plot(th,G(:,Nph/2),'k-');

xlabel('Elevation angle, theta (degrees)');

ylabel('Realized gain (in dBi)');

title('H-plane gain for a slotted waveguide antenna.');

text(25,1.1*maxG,['Numerical realized gain = ', num2str(maxG,4),' dBi.']);

text(35,maxG,['On boresight phi = ', num2str(ph(Nph/2),3),' degrees.']);

figure(5);

plot(ph,G(bw0,:));

xlabel('Azimuthal angle, phi (degrees)');

ylabel('Realized gain (in dBi)');

title('E-plane gain for a slotted waveguide antenna.');

text(25,1.1*maxG,['Numerical realized gain = ', num2str(maxG,4),' dBi.']);

text(35,maxG,['At main-beam-angle, theta0 = ', num2str(th(bw0),3),' degrees.']);

%%%%%%%%%%%%%%%%%%%%%%%%%%%%%%%%%%%%%%%%

['Total clock time is ', num2str(toc/60,3),' minutes.'],

%ONEDWAVE is a non-uniform t-line code using FEM as in Jin
```

```
%INPUT AXIAL PROPAGATION CONSTANT AND FEM PARAMETERS

% 4/00 function [phi]= onedfem(beta0,M,dz,Z10,ZH);

%Uses onedfem to solve for TE wave propagation (Jin p.54)

%for non-uniform T-line in axial direction w/o sources so f=0

%Using M finite element cells and linear interpolation N=M+1;

%Element lengths constant mesh l=ones(M,1)*dz;

%BVP parameters for non-uniform T-line propagation alpha=-1./beta0./ZH;
beta=beta0./ZH;

%B.C. from T-line eqs for reflection and transmission at terminal planes

gammaL=-i/ZH(N); qL=0;

gamma0=-i/Z10; q0=-2*i/Z10;

%%%%%%%%%%%%%%%%%%%%%%%%%%%%%%%%%%%%%%%%%%%%%%%%%%%%%%%%%%%%%%%%%%%%%%%%%%%%%%%%

%Solves a 1-D BVP using FEM for M elements using Jin notation

%Solution (phi=V or I) Subject to mixed (or Neuman) B.C. at

%at z=0 -alpha*dE/dx+gamma*E=q and at z=L alpha*dE/dx+gamma*E=q

%Setup interaction matrix size NxN

K(1)=alpha(1)/l(1) + beta(1)*l(1)/3;

K(N)=alpha(M)/l(M) + beta(M)*l(M)/3;

for n=2:N-1;

K(n)= alpha(n-1)/l(n-1) + beta(n-1)*l(n-1)/3 + ...
```

```
alpha(n)/l(n) + beta(n)*l(n)/3;

end

for m=1:N-1;

C(m)=-alpha(m)/l(m) + beta(m)*l(m)/6;

end

%%%%%%%%%%%%%%%%%%%%%%%%%%%%%%%%%%%%%%%%

for k=1:N; b(k)=0; end;

%Enforce Mixed (or Neuman) B.C. at x=0

K(1)=alpha(1)/l(1) + beta(1)*l(1)/3 + gamma0;

b(1)=q0;

%Enforce Mixed (or Neuman) B.C. at x=L

K(N)=alpha(M)/l(M) + beta(M)*l(M)/3 + gammaL;

b(N)=qL
%%%%%%%%%%%%%%%%%%%%%%%%%%%%%%%%%%%%%%%%

%Solve system for V(z): slash uses Gaussian Elimination for k = 2:N;

K(k) = K(k) - (C(k - 1)^2/K(k - 1));

b(k) = b(k) -(C(k-1)*b(k-1)/K(k-1));

end %%%%%%%%%%%%%%%%%%%%%%%%%%%%%%%%%%%%%%%%

phi(N)=b(N)/K(N);

for p=1:N-1;
```

```
k=N-p; phi(k) = (b(k) - (C(k)*phi(k+1)))/K(k);

end;

K=0;C=0;

%%%%%%%%%%%%%%%%%%%%%%%%%%%%%%%%%%%%%%%
```

Distribution

Admnstr
Defns Techl Info Ctr
ATTN DTIC-OCP
8725 John J Kingman Rd Ste 0944
FT Belvoir VA 22060-6218

DARPA
ATTN S Welby
3701 N Fairfax Dr
Arlington VA 22203-1714

Ofc of the Secy of Defns
ATTN ODDRE (R&AT)
The Pentagon
Washington DC 20301-3080

AMCOM MRDEC
ATTN AMSMI-RD W C McCorkle
Redstone Arsenal AL 35898-5240

US Army TRADOC
Battle Lab Integration & Techl Dirctrt
ATTN ATCD-B
FT Monroe VA 23651-5850

US Military Acdmy
Mathematical Sci Ctr of Excellence
ATTN MADN-MATH MAJ M Johnson
Thayer Hall
West Point NY 10996-1786

Dir for MANPRINT
Ofc of the Deputy Chief of Staff for Prsnnl
ATTN J Hiller
The Pentagon Rm 2C733
Washington DC 20301-0300

SMC/CZA
2435 Vela Way Ste 1613
El Segundo CA 90245-5500

TECOM
ATTN AMSTE-CL
Aberdeen Proving Ground MD 21005-5057

US Army ARDEC
ATTN AMSTA-AR-TD
Bldg 1
Picatinny Arsenal NJ 07806-5000

US Army Info Sys Engrg Cmnd
ATTN AMSEL-IE-TD F Jenia
FT Huachuca AZ 85613-5300

US Army Natick RDEC Acting Techl Dir
ATTN SBCN-T P Brandler
Natick MA 01760-5002

US Army Simulation Train & Instrmntn Cmnd
ATTN AMSTI-CG M Macedonia
ATTN J Stahl
12350 Research Parkway
Orlando FL 32826-3726

US Army Tank-Automtv Cmnd RDEC
ATTN AMSTA-TR J Chapin
Warren MI 48397-5000

Hicks & Assoc Inc
ATTN G Singley III
1710 Goodrich Dr Ste 1300
McLean VA 22102

Palisades Inst for Rsrch Svc Inc
ATTN E Carr
1745 Jefferson Davis Hwy Ste 500
Arlington VA 22202-3402

Director
US Army Rsrch Lab
ATTN AMSRL-RO-D JCI Chang
ATTN AMSRL-RO-EN W D Bach
PO Box 12211
Research Triangle Park NC 27709

US Army Rsrch Lab
ATTN AMSRL-CI-IS-R Mail & Records Mgmt
ATTN AMSRL-CI-IS-T Techl Pub (2 copies)
ATTN AMSRL-CI-OK-TL Techl Lib (2 copies)
ATTN AMSRL-SE-DE C Reiff
ATTN AMSRL-SE-DS J Miletta
ATTN AMSRL-SE-DS W O Coburn
(20 copies)
ATTN AMSRL-D D R Smith
ATTN AMSRL-DD J M Miller
Adelphi MD 20783-1197

REPORT DOCUMENTATION PAGE

Form Approved
OMB No. 0704-0188

1. AGENCY USE ONLY *(Leave blank)*	2. REPORT DATE	3. REPORT TYPE AND DATES COVERED
	September 2001	Final, June–September 2000

4. TITLE AND SUBTITLE Design Procedure for a Frequency-Scanned Traveling Wave Antenna, Part I: Air-Filled Waveguide

5. FUNDING NUMBERS
DA PR: A140
PE: 62120A

6. AUTHOR(S) William Coburn (ARL), Wasyl Wasylkiwskyj (George Washington University)

7. PERFORMING ORGANIZATION NAME(S) AND ADDRESS(ES)
U.S. Army Research Laboratory
Attn: AMSRL-SE-DS email: wcoburn@arl.army.mil
2800 Powder Mill Road
Adelphi, MD 20783-1197

8. PERFORMING ORGANIZATION REPORT NUMBER
ARL-TR-791

9. SPONSORING/MONITORING AGENCY NAME(S) AND ADDRESS(ES)
U.S. Army Research Laboratory
2800 Powder Mill Road
Adelphi, MD 20783-1197

10. SPONSORING/MONITORING AGENCY REPORT NUMBER

11. SUPPLEMENTARY NOTES
ARL PR: 0NEYYY
AMS code: 622120.140

12a. DISTRIBUTION/AVAILABILITY STATEMENT Approved for public release; distribution unlimited.

12b. DISTRIBUTION CODE

13. ABSTRACT *(Maximum 200 words)*

A leaky waveguide antenna is investigated through a combination of theoretical analysis and numerical simulation. We developed a design procedure based on the analysis of Goldstone and Oliner for an aperture in the narrow wall of a rectangular waveguide. We can phase scan the antenna by adjusting the propagation constant of the guiding structure, and we can frequency scan it by taking advantage of frequency dispersive behavior. A combination of frequency and phase scanning can be used to steer the beam. We describe how the aperture illumination function is synthesized for a constant width aperture and we present the design equations. We use a numerical simulation of the leaky waveguide section to obtain the radiation efficiency. We then calculate the realized gain to evaluate the frequency scan range and radiation pattern characteristics. The results demonstrate that the main beam position can be scanned in the range of 10° to 30° from broadside over a narrow frequency range without corrupting the radiation pattern.

14. SUBJECT TERMS Frequency scan, phase scan, leaky wave antenna, traveling wave antenna

15. NUMBER OF PAGES 73

16. PRICE CODE

17. SECURITY CLASSIFICATION OF REPORT	18. SECURITY CLASSIFICATION OF THIS PAGE	19. SECURITY CLASSIFICATION OF ABSTRACT	20. LIMITATION OF ABSTRACT
Unclassified	Unclassified	Unclassified	UL

NSN 7540-01-280-5500

Standard Form 298 (Rev. 2-89)
Prescribed by ANSI Std. Z39-18
298-102